Studies on the audition-independent vocal development in songbird

(ソングバードを用いた聴覚非依存的な発声パターンの発達に関する研究)

A DISSERTATION
Submitted to the Graduate School of Life Science,
Hokkaido University

In partial fulfillment of the requirements for the degree
DOCTOR OF LIFE SCIENCE

Chihiro Mori

2015

Contents

General Introduction

Many animals communicate with each other by vocalization. Although the vocalizations of most animal species are innate, few groups of animals such as mammals (humans, cetaceans, bats, elephants, and pinnepeds) and birds (oscine songbirds, parrots, and hummingbirds) (Janik and Slater, 1997; Javis, 2004; Poole et al., 2005) develop a complex vocal pattern through vocal learning. The songbird is an attractive animal model for understanding the mechanisms underlying vocal learning because non-human primates and rodents have a limited ability to modify their vocalization (Egnor and Hauser, 2004; Mahrt et al., 2013). There are approximately 3,500 songbird species throughout the world. Their birdsong shows a readily quantifiable species-specific variation, ideal to investigate the developmental changes in acoustic structures and their sequences. Some species of birds such as the zebra finch and canary are easily bred under laboratory conditions, while others are not always easily bred.

In addition to the aforementioned advantages to study vocal learning, the birdsong is similar to human speech in the following three aspects (Doupe and Kuhl, 1999), although birds and mammals have diverged from a common ancestor approximately three hundred million years ago (Jarvis et al., 2005).

First, sensory and sensorimotor learning is crucial for the development of both the birdsong and human speech (Doupe and Kuhl, 1999). Sensory learning is the initial phase. Animals listen to and memorize conspecific adult vocalization as their template. The sensorimotor learning follows, and animals start vocalizing, gradually matching their vocalization to the memorized template. At the early stage of sensorimotor learning, fledgling juvenile songbirds produce unstructured sounds. These sounds are referred to as subsong. The subsong is similar to the babbling vocalization of human infants. Juveniles compare these sounds with the memorized

template and achieve vocal imitation through a process of trial-and-error vocalizations using auditory feedback.

Second, the learned vocalizations consist of a complex motor sequence, which is quantified in terms of phonology and syntax in both songbirds and humans. Although the human speech and birdsong share common features and their vocal patterns are defined as ordered strings of sounds, they are different in a critical character. While the human speech can flexibly convey different meanings when words are associated in distinct orders, the birdsong conveys signals for territorial advertisement and for mate attraction and information about the individual identity.

Third, vocal learning occurs within a critical period, usually at the early developmental stage before adulthood. Both songbirds and humans are unable to learn vocalization equally well throughout their life. Although it is critical that humans and birds are provided with appropriate auditory and social conditions during the critical period to achieve vocal learning, they are different with regard to the following point: humans are able to learn new words and languages throughout their life. Some species of songbirds categorized as closed-ended vocal learners, e.g., the zebra finch and Bengalese finch, which are commonly used in research, are unable to learn new songs at the adult stage, while others categorized as open-ended vocal learners, e.g., the canary, have the ability to imitate new sounds to some extent as adults.

The process of vocal learning and the critical period in songbirds were revealed through laboratory studies such as auditory deprivation and social isolation (Konishi, 1964; Marler, 1970). Actually, many species of songbirds raised in auditory deprivation or complete social isolation develop abnormal songs (Konishi, 1964, 1965, 1985; Nottebohm, 1968; Marler et al., 1972; Marler and Waser, 1977; Price, 1979; Marler and Sherman, 1983). Audition provides important information for learning, both for memorizing model songs and precisely evaluating

the bird's own vocal output.

Although the auditory input is crucial for acquiring complex vocal patterns, its exact role in neural circuit maturation for vocal learning and production is not well understood. In my thesis, I studied vocal development in songbirds, focusing on the auditory input as developmental epigenetic factor for vocal learning. The term "epigenetic factor" in my study refers to experiences that affect behavior via epigenetic modifications that alter DNA transcription in neurons (Riccio, 2010; Meaney and Ferguson-Smith, 2010). To examine how auditory deprivation affects developmental gene expression in major elements of neural circuits mediating vocal learning and production, I compared the development of the song and gene expression pattern between intact and audition-deprived songbirds.

Accumulated studies in diverse animal models have demonstrated that sensory experience is required for normal functional and structural maturation of brain circuits (Hubel and Wiesel, 1970; Van der Loos and Woolsey, 1973; Holtmaat and Svoboda, 2009). Interestingly, dark rearing and monocular deprivation during the critical period alter the patterning of synaptic connectivity within the visual cortex (Hubel and Wiesel, 1970). Manipulation of the visual input also regulates the expression of genes required for this visual cortex maturation (Majdan and Shatz, 2006; Hensch, 2004). Similarly, modulating the somatosensory input to the barrel cortex by trimming whiskers changes the formation of cortical barrels (specialized cortical structures found in the rodent somatosensory cortex) and the response properties of the residing cortical neurons (Van der Loos and Woolsey, 1973; Erzurumlu and Gaspar, 2012).

These previous findings on the mechanisms underlying experience-dependent circuit maturation have notably been produced using sensory deprivation. Comparing the intact and sensory deprived animals provides insight into the influence of external stimuli and intrinsic-driven neurological processes. The development of neural circuits for visual and

somatosensory systems mainly depends on the sensory input; however, neural circuits for vocal learning and production develop through the interplay between the auditory input and vocal motor output. Therefore, I reasoned that studying audition-deprived songbirds could uncover intrinsic-motor driven processes in the absence of pathological abnormalities.

In the first chapter, to investigate how early-deafened birds develop their song over a long period of time, I deafened birds before the initiation of sensory learning. Although several deafening experiments have been performed in many songbird species (Konishi, 1964, 1965, 1965; Nottebohm, 1968; Marler, et al., 1972; Marler and Waser, 1977; Price, 1979; Marler and Sherman, 1983), little attention has been paid to the timing of song stabilization following auditory deprivation. First, I analyzed whether the songs of early-deafened zebra finches stabilized. The zebra finch, a closed-ended learner, develops a readily quantifiable song and crystallizes a stereotyped song. I found that the early-deafened birds required twice as much time as the hearing-intact birds to stabilize a song pattern. Then, to examine whether the song also crystallizes under audition deprived condition in the open-ended learner, I observed song development of early deafened canary. Although there is the species difference in the contribution of auditory input to crystallize song between the closed-ended and open-ended vocal learner, the results indicated that song stabilization occur audition independently.

In the second chapter, I quantified the neural activity during singing in the brain areas associated with song learning and production to examine where auditory deprivation affects the neural circuits. Song production and learning are controlled by two major circuits: the posterior vocal motor circuit and the anterior basal ganglia–forebrain circuit. The vocal motor circuit is involved in producing vocal patterns (Yu and Margoliash, 1996; Hahnloser et al., 2002). The basal ganglia–forebrain circuit in songbirds plays a critical role in song learning by producing vocal exploration (Bottjer et al., 1984; Scharff and Nottebohm, 1991; Kao et al., 2005;

Andalman and Fee, 2009). The results indicated that the neural activity of song nuclei in both circuits was similar between the intact and early-deafened birds throughout development. In addition, I reported the possibility that the basal ganglia–forebrain circuit is involved in generating the song pattern without auditory information.

In the third chapter, I performed global transcriptome analysis in the vocal motor circuit during song development to investigate whether hearing loss, which may cause delayed song crystallization in early-deafened birds, affects the developmental gene expression profile. I found that developmental gene expression in the motor circuit changes in an age-dependent manner from the juvenile to older adult stage, even in the deafened birds, in contrast to different rates of song development between the intact and deafened birds. Moreover, I showed that, even after adult deafening, which degrades crystallized song, the deteriorated songs ultimately re-stabilized at the same point when the early-deafened birds stabilized their songs. These results indicate a genetic program-associated inevitable termination of vocal plasticity that results in audition-independent vocal crystallization.

Based on these results, I discuss hypotheses on two different mechanisms underlying song crystallization: “audition-dependent” and “audition-independent” song crystallization. These two modes are referred to as “active” and “passive” mode in my hypothesis. “Active” song crystallization is the traditional song crystallization maintained by auditory information. In contrast, volitional vocalization as a motor activity can be a crucial epigenetic factor that drives the genetic programs to regulate vocal plasticity and develop vocal patterns for “passive” song crystallization.

Chapter I

Song Development and Stabilization in Early-Deafened Songbirds

1.1 Introduction

The birdsong, like human speech, is a complex vocal behavior acquired through sensorimotor learning. Developmental epigenetic factors such as social interaction (Kroodsma and Pickert, 1984) and nutrition (Nowicki et al., 2002) influence vocal learning. In addition, an auditory input is crucial for the acquisition of the birdsong and human speech as an epigenetic factor for sensorimotor learning (Konishi, 1965; Ruben, 1997). Audition provides important information for vocal learning, both for hearing model songs and for the precise evaluation of the own vocal output. However, audition-deprived songbirds can still develop a certain degree of species-specific song, albeit noisy and amorphous (Price, 1979; Marler, 1983). This suggests that an inherited genetic predisposition also contributes to song development and the generation of song patterns; however the mechanism by which the auditory input regulates the genetic programs in neural substrates mediating the development and stabilization of complex vocal patterns remains unclear. In the present study, to determine the role of auditory feedback for song development, I used early-deafened songbirds, the zebra finch and canary, with sensorineural hearing loss, focusing on how the song develops and when it crystallizes without auditory information.

The zebra finch is known as a closed-ended learner of complex vocal patterns, given that once a stable song pattern "motif" is developed, the song structure remains unchanged throughout life (Immelmann, 1969; Eales, 1985; Zann, 1996). This stereotypy of crystallized song enables the precise quantification of the similarities and differences in vocal development and song patterns between the intact and deafened birds, thereby allowing the examination of how genetic and epigenetic factors contribute to the acquisition and maintenance of complex vocal patterns. I showed that the early-deafened zebra finches can still develop crystallized songs, albeit more slowly than the intact birds.

In contrast to some species of songbirds categorized as closed-ended vocal learners, e.g., the zebra finch, others categorized as open-ended vocal learners, e.g., the canary, have the ability to imitate new sounds to some extent as adults. I therefore examined how auditory deprivation affects the vocal development in the canary that possesses different properties of song plasticity to the closed-ended learner. I found that early-deafened canaries can develop crystallized songs in a time course similar to that of intact canaries. In addition, I observed that song degradation was seasonally induced. Following this, the song re-crystallized in a song pattern similar to the first crystallized pattern, like the hearing-intact canary.

These results provide evidence for the audition-independent regulation of vocal development and crystallization, although the auditory input has a more significant contribution to the timing of normal song crystallization in the zebra finch than in the canary.

1.2 Materials and Methods

Animals

I used male zebra finches (*Taeniopygia guttata*) from our breeding colony and male canaries (*Serius canaria*) at the Rockefeller University Field Research Center. The photoperiod was constantly maintained at a 14:10 h light/dark cycle for the zebra finches and corresponded to that of New York State for the canaries. Food and water were available *ad libitum* throughout the year. The sex of birds was checked by PCR as previously reported (Wada et al., 2006) before the start of sensory learning (the zebra finch: within three days after hatching, the canary: until days post hatching; dph 35). The birds were raised in individual breeding cages with their parents and siblings until at least dph 30 and were then housed in single-sex groups (6–10 birds per cage) with visual and auditory access to both the male and female birds. I divided zebra finches into the following developmental stages to examine age-associated changes: dph 47–65 (juvenile), dph 100–187 (young adult), and >dph 300 (older adult). For social isolation, the juvenile zebra finches were separated from their fathers by dph 5 and raised by their mothers with their siblings in a sound-attenuation box until they could feed themselves (dph 35). No song tutor was provided, and they could not see the other zebra finches or hear other songs after dph 35. All animal experiments were performed according to the guidelines of the Committee on Animal Experiments of Hokkaido University from whom permission for this study was obtained and the Rockefeller University Institutional Animal Care and Use Committee.

Song recording and analysis

The birds were individually housed in sound-attenuation boxes. Songs were automatically saved 24 h per day using the Sound Analysis Pro program (v1.04) (Tchernichovski et al., 2000) at 16 bits and a 44 kHz sampling rate. Analysis of syllable

acoustic structure was performed using Sound Analysis Pro and Avisoft Saslab (Avisoft Bioacoustics). Low- and high-frequency noises (<0.5 kHz and >1.9 kHz) were filtered from the recordings using Avisoft Saslab, and the low frequency noises (<1.5 kHz) were further filtered using Sound Analysis Pro. For all analyses, I randomly selected songs per time-point and manually eliminated calls and cage noise from the dataset. The entropy and amplitude parameters of syllables were set manually, and the syllables were segmented using Sound Analysis Pro. A song bout was defined as the continuous production of syllables followed by at least 400 ms of silence. Typical song bouts in adult zebra finches start with introductory notes followed by one or more motifs that consist of the same stereotyped sequence of syllables.

To measure the degree of song stabilization, I calculated song similarity by the Kullback–Leibler (K-L) distance analysis (Wu et al., 2008) between song at each developmental stage and at >1 year of age. The K-L distance analysis compares the probability density function from two large sets of syllables and quantifies the difference. Syllable density scatter plots were treated as random samples from a two-dimensional probability distribution. For construction of two-dimensional scatter plots with syllable duration and mean frequency modulation (mFM), I used 600–1000 syllables (mean ± SD; 982 ± 68) at each developmental stage for each bird. The two-dimensional scatter plot was partitioned into an M by N array of bins (syllable duration is partitioned into M=13 equally-spaced bins; 40 ms and mFM is partitioned into N=10 equally-spaced bins; 10). To obtain an accurate and consistent estimation of the distribution, M and N were kept constant throughout all days of singing. The number of data points in each bin was counted and divided by the total number of points in the plot. I represented the two-dimensional scatter plot generated at >1 year of age by P_s and the scatter plot at each developmental stage as P_k. The difference between P_s and P_k was calculated to obtain the estimate probability density functions (denoted Q_s and Q_k) for the two scatter plots. The K-L

distance is represented by the following equation:

$$D_{KL}(Q_s \| Q_k) = \sum_{m=s}^{M} \sum_{n=s}^{N} q_s(m,n) \log_2 \frac{q_s(mn)}{q_k(mn)},$$

where q_s (m, n) and q_k (m, n) denote the estimated probabilities for bin (m, n). Large values of the K-L distance indicate that the two patterns are more dissimilar, whereas a K-L distance of 0 indicates a perfect match. I normalized the K-L distance value to the average K-L distance at the first stage of development (dph 49–59) for each experimental group. I used 15 male zebra finches (intact: *n* = 4; early-deafened: *n* = 6; socially isolated: *n* = 5) for the K-L distance analysis.

In order to compare similarity among syllables in a motif, I used avisoft-CORRELATOR and made sound-similarity-matrixes of spectrograms. All selected spectrograms of syllables were compared with each other. Each comparison was performed by sliding two spectrograms of syllables along the time axis. For every offset position, the correlation coefficient was computed according to the following formula:

$$\Phi_{XY} = \frac{\sum_X \sum_Y ((a_{xy} - m_a) * (b_{xy} - m_b))}{\sqrt{\sum_X \sum_Y (a_{xy} - m_a)^2 * \sum_X \sum_Y (b_{xy} - m_b)^2}},$$

where m_a and m_b are the mean values of the spectrograms. a_{xy} and b_{xy} are the intensities of the spectrogram points at the locations x,y. The correlation coefficient is a value ranging from -1 to +1. A value 1 means that the two spectrograms are identical. A value 0 means that there is no similarity between the spectrograms. Values below zero occur when the two spectrograms are inversed. The peak value of the correlation coefficients was saved in a correlation matrix as the score of syllable similarity.

Measurement of testosterone levels

I measured the serum concentration of circulating testosterone in the male juveniles (n = 16, 8/group), young adults (n = 20, 10/group), and older adults (n = 20, 10/group) to examine whether early stage deafening affects the rate of maturation. Blood was sampled before lights on (morning) under silent conditions. Blood serum was isolated by centrifuging whole blood for 15 min at RT and was stored at −30°C until testosterone analyses. The blood serum samples were diluted by ARCHITECT Testosterone Manual Diluent (Abbott Laboratories) and testosterone levels were measured by BML, Inc (Tokyo, Japan).

Deafening

The birds were deafened by cochlear extirpation at dph 17–23 (before fledging) for the zebra finches and dph 24-34 for the canaries to establish the early-deafened group. The birds were anesthetized with pentobarbital (6.48 mg/ml; 60 μL/10 g of body weight) by intra peritoneal injection. After fixing the head in a custom-made stereotaxic apparatus with ear bars, a small window was made through the neck muscle and the skull near the end of the elastic extension of the hyoid bone. A small hole was then made in the cochlear dome. The cochlea was pulled out with a fine hooked wire. The removed cochleae were confirmed by visual inspection under a dissecting microscope. After bilateral cochlear removal, the birds were put back in their nest and kept with their parents and siblings until at least dph 30.

1.3 Results

To examine how a song developed and the characteristic song patterns under an audition-deprived condition, the male zebra finches were deafened by removing the cochleae before fledging [days post-hatching (dph) 18–22; average dph 19; n = 6], a time during which no song production is observed, and song ontogeny was compared in the intact and socially isolated birds (n = 4 and 5, respectively). Zebra finch is close-ended learner which learns song once during the early stage of the first year and then repeat learned one song pattern in a stereotyped manner for the rest of his life. This feature is advantageous for analysis of audition-deprived effect on vocal development. Because of sensorineural hearing loss, the songbirds missed listening to song models and monitoring their own vocal outputs. These early-deafened zebra finches showed slower song development than the intact and socially isolated birds. Clear differences in song development were observed at dph 140–180; during this period, the majority of the intact zebra finches exhibited crystallized song patterns (**Fig. I-1*A*, Fig. I-2**). In contrast, the early-deafened zebra finches still generated variable song sequences with fewer harmonic syllables, resembling the early plastic songs recording during early normal development. However, the deafened zebra finches eventually exhibited stabilized song patterns characterized by stable temporal sequences of distinguishable syllables by approximately dph 300, which is approximately three times longer than the time required for song crystallization in the intact birds (**Fig. I-1*C*, I-2**). There was a significant difference in the degree of song stabilization between the early-deafened and intact zebra finches at dph 140–180 (Student's t test with Bonferroni correction, $p < 0.01$) (**Fig. I-2**). Although there was no significant difference in the song stabilization trajectory between the socially isolated and early-deafened birds, the socially isolated birds exhibited a tendency for generating "parts" of a motif structure and stabilizing the acoustic features for the majority of syllables with a time course similar to

that in the intact birds (**Fig. I-1*A, B***: syllable scatter plots). In contrast, all the early-deafened zebra finches continued to generate acoustically unstable syllables across bouts, and their stable motif patterns did not emerge at dph140-180. During the developmental period prior to song crystallization/stabilization, circulating testosterone concentration and singing frequency were not significantly different between the intact and early-deafened birds (**Fig. I-3**). Furthermore, it was also observed that the early-deafened birds directed songs to females and exhibited normal mating behavior at approximately dph 100, the typical time of sexual maturity, suggesting that delayed song stabilization in the early-deafened birds did not generally reflect retardation in development.

The stabilized songs of the deafened birds were composed of a motif structure showing a variety of individual differences in the number of syllables, acoustic features, syllable durations, and intersyllabic intervals (**Fig. I-1*C***, **I-4**). These individual differences were observed even among siblings from the same family (**Fig. I-4**). To examine whether any general rules exist in diverse song patterns of deafened birds, I measured the motif duration, syllable duration, number of syllable in a motif, and syllable similarity. I calculated the mean value of motif duration for each deafened bird, and found some rules (**Fig. I-5**). The duration of the motif-like song pattern was generally short (mean duration = 0.88 sec) and constant. In comparison, the duration of repetitive song pattern was longer (mean duration = 1.37 sec) and variable. These results indicate that hearing loss at an early developmental stage delayed but did not prevent the eventual slow development of some stable syllables and structured vocal sequences which showed individual differences. The individual differences developed with innate constraints.

Following this, I performed audition deprivation for canaries to examine whether the song stabilizes independently to audition in open-ended learners. Although the canary crystallizes song during the late winter of the first year, song instability recurs every early fall

after the end of the breeding season and is followed by a stable song with new syllable addition and loss of some earlier syllables in the winter (**Fig. I-6**). I considered the possibility of audition deprivation preventing song crystallization or seasonal plasticity. However, the early-deafened canaries showed song development similar to that of intact birds and produced a stabilized song similar to that in the first year without auditory feedback following a plastic song in the second year (**Fig. I-6**). This result indicated that the annual cycle of song instability and crystallization in the canary is regulated independently of audition.

Although the degree of contribution of the auditory experience to song development was species-specific between closed-ended learners and open-ended learners, these results indicated that song stabilization was regulated independently of audition. I observed that individual variability in the vocal pattern was much higher in early-deafened zebra finches. Some early-deafened birds develop a species-specific song structure similar to a motif pattern, while others develop repetitions with long–duration bouts (**Fig. I-4, I-6**). A song with repetitive syllables is hardly observed in hearing-intact zebra finches (**Fig. I-4, I-5**). This result suggested that auditory information enhanced bias to species-specificity of songs with genetic predisposition.

1.4 Discussion

Vocal learning is a complex form of sensorimotor learning which is based on the coordination between the sensory input and motor output to guide vocalization. Complex learned vocalization is shaped by both genetic and environmental influences.

My study revealed audition-independent vocal development and stabilization in the zebra finch and canary. The early-deafened zebra finches stabilized their song with individual differences, and the timing of song stabilization was delayed in comparison with that in intact zebra finches. The early-deafened canaries developed and crystallized their song in a manner as similar to that in the intact canaries. These results suggest that although there is a species difference in the auditory contribution to song development, song stabilization is caused not only by auditory-dependent learning but also by the innate genetic program. In addition, the positive correlation between the motif duration and syllable similarity (motif or repetition) in early-deafened zebra finches suggested an innate constraint of the song pattern.

The assessment of singing frequency revealed that hearing loss did not affect the amount of vocalization in the zebra finch. Although several factors (e.g., hormone level and feedback of peripheral nerves) may be involved in vocal development, this result suggests that singing mainly drives the innate genetic program to reduce vocal plasticity.

The zebra finch requires an auditory input to crystallize the stereotyped song structure at an appropriate timing to breed soon after sexual maturation. In the canary, an open-ended learner, my result suggested that the regulation of song plasticity does not depend on auditory feedback. Testosterone is known to be involved in song plasticity (Marler et al., 1988; Alliende et al., 2010) and shows seasonal changes in circulating levels in the canary (Nottebohm et al., 1987). These facts indicate that the contribution of auditory feedback and other factors (e.g., hormones) of song stabilization is differs between species of closed-ended learners and

open-ended learners.

1.5 Figures

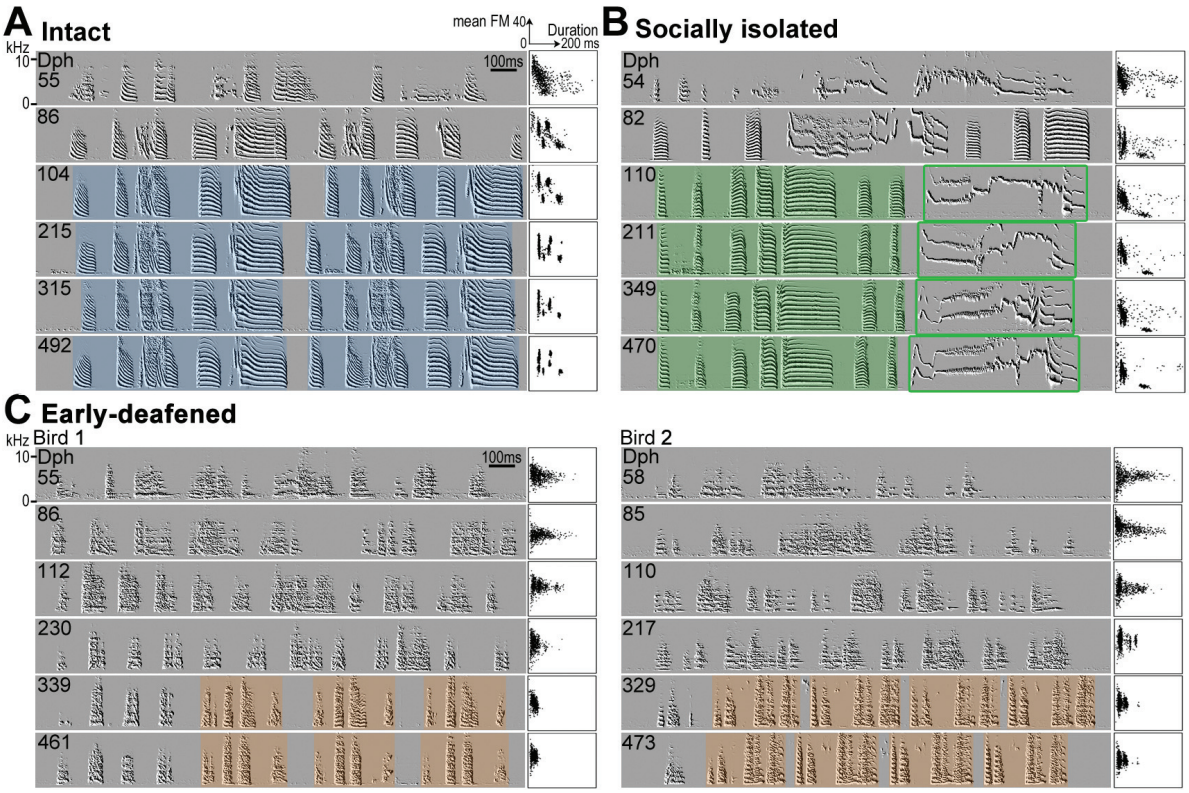
A Intact
mean FM 40
0
Duration
200 ms
kHz
10
0
Dph
55
100ms
86
104
215
315
492
B Socially isolated
Dph
54
82
110
211
349
470
C Early-deafened
kHz
Bird 1
10
0
Dph
55
100ms
86
112
230
339
461
Bird 2
Dph
58
85
110
217
329
473

Figure I-1. Comparison of song development and stabilization in intact, socially isolated, and early-deafened zebra finches.

***A*, *B*,** Examples of song development and syllable scatter plots (duration versus mean FM) in an intact (*A*) and a socially isolated bird (*B*). Color shadings (blue and green) highlight stable song motifs. The intact and socially isolated birds exhibited song stability around dph 110. The crystallized song pattern of the socially isolated bird is similar to that of the intact (normal) bird, except for a prolonged and variable syllable (green bracket).

***C*,** Examples of song development and syllable scatter plots (duration versus mean FM) in two early-deafened zebra finches. Orange shading highlights stable song motifs.

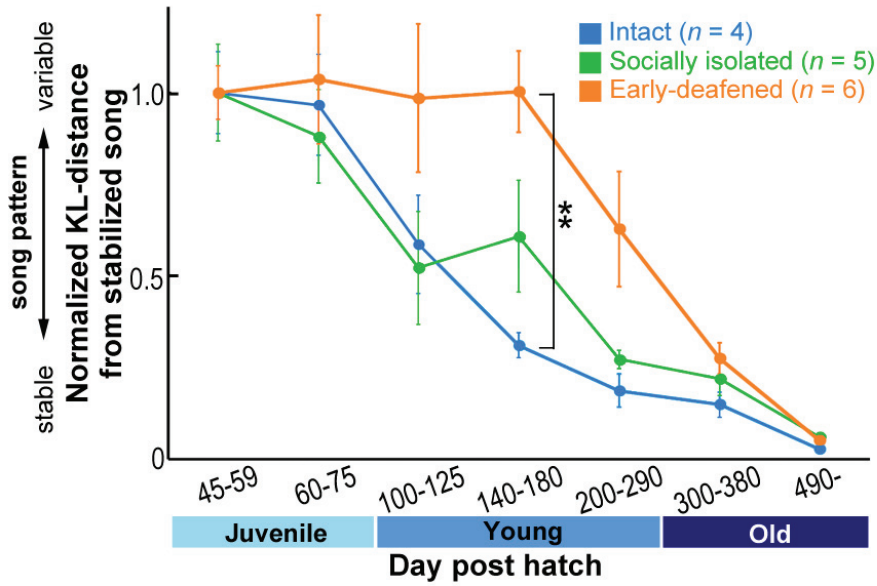
Intact (n = 4)
Socially isolated (n = 5)
Early-deafened (n = 6)
song pattern
variable
stable
Normalized KL-distance from stabilized song
1.0
0.5
0
**
45-59
60-75
100-125
140-180
200-290
300-380
490-
Juvenile
Young
Old
Day post hatch

Figure I-2. Normalized Kullback–Leibler (K-L) distance calculated from the last syllable scatter plot representing crystallized/stabilized song patterns.

The values of K-L distance at dph 45–59 are normalized as 1.0. A value near 0 indicates a crystallized/stabilized song pattern. Mean ± SEM (intact: $n = 4$; socially isolated: $n = 5$; early-deafened: $n = 6$; Student's t-test with Bonferroni correction, $^{**}p < 0.01$).

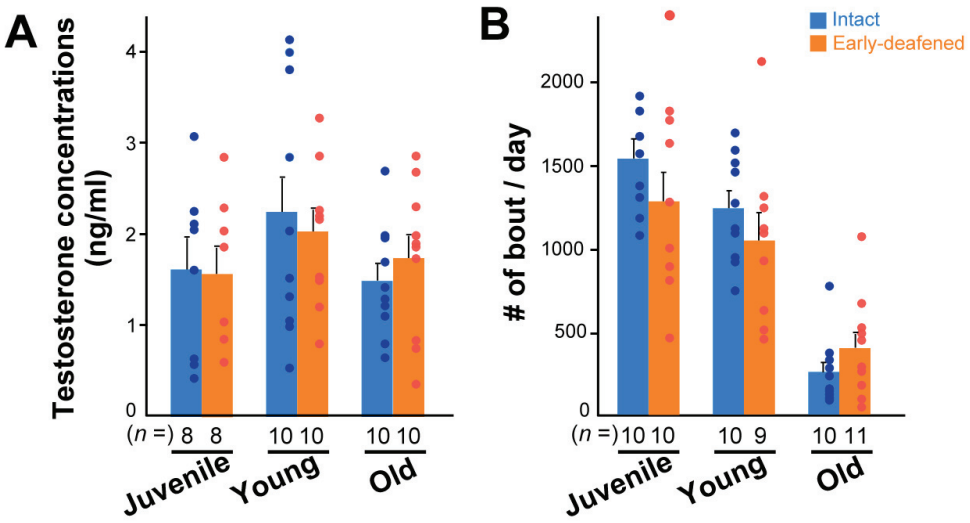
A
Testosterone concentrations (ng/ml)
0
1
2
3
4
(n =) 8 8
10 10
10 10
Juvenile
Young
Old
B
Intact
Early-deafened
# of bout / day
0
500
1000
1500
2000
(n =) 10 10
10 9
10 11
Juvenile
Young
Old

Figure I-3. Delayed song stabilization in the early-deafened birds was not caused by immature development.

***A*,** Average levels of circulating testosterone at three developmental stages, juvenile (dph 50–60), young (dph 105–130), and old (> dph 330), in intact (blue bars) and early-deafened (orange bars) birds. No significant difference was observed in serum testosterone between the two groups at any developmental stage. Each dot and bar represents individual values and mean ± SEM, respectively, of testosterone concentrations (ng/ml). Each animal number is indicated under the bar.

***B*,** Average number of song bouts/day during the three developmental periods, juvenile (dph 60–65), young (dph 100–110), and old adult (dph 440–920) in intact (blue bars) and early-deafened (orange bars) zebra finches. Comparison of intact and early-deafened birds indicates no significant difference at each stage (juvenile: $p = 0.236$; young: $p = 0.352$; old: $p = 0.237$; Student's t test). Each dot and bar represents individual values and the mean ± SEM, respectively. Each animal number is indicated under the bar.

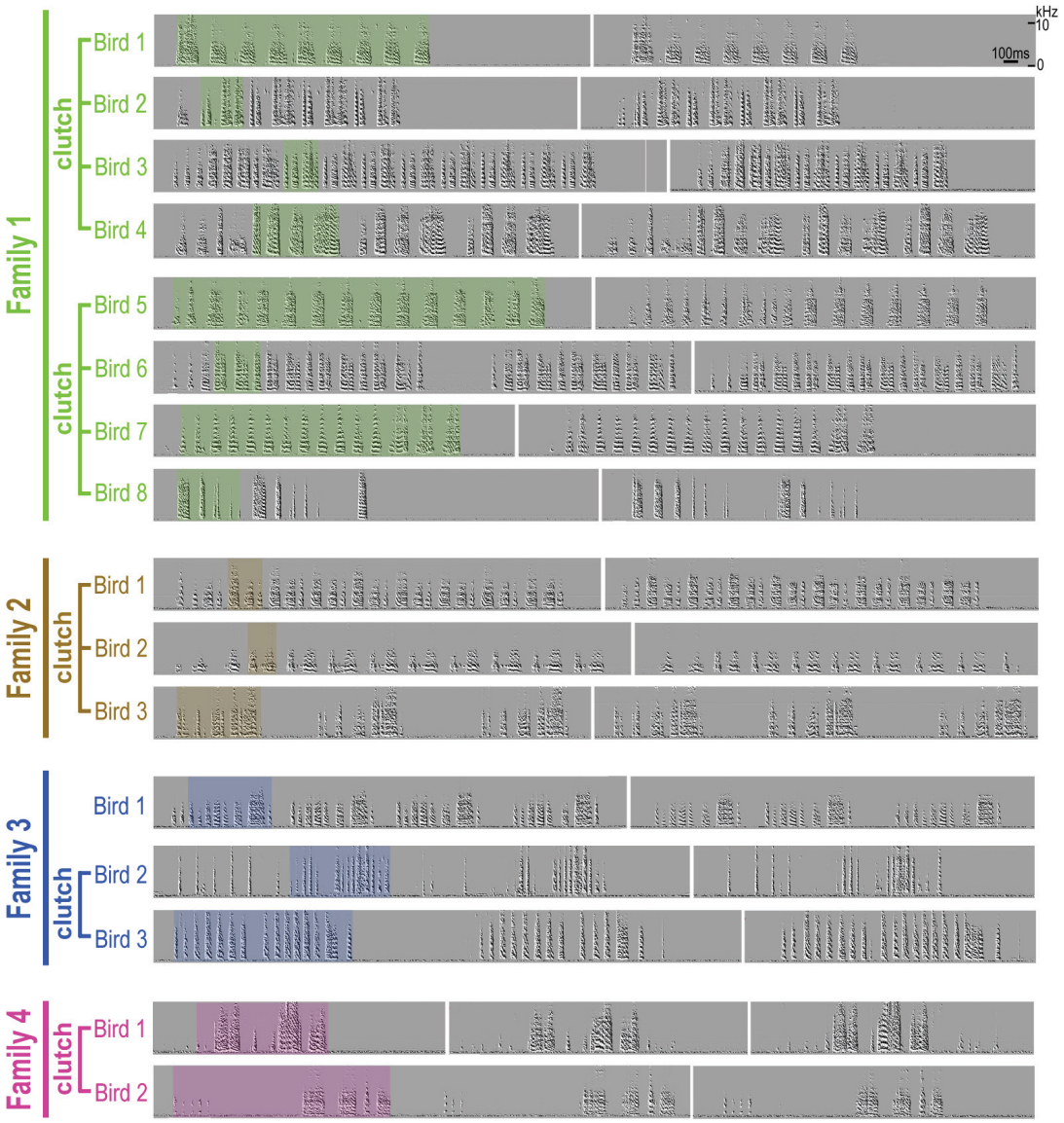
Family 1
clutch
Bird 1
Bird 2
Bird 3
Bird 4
clutch
Bird 5
Bird 6
Bird 7
Bird 8
kHz
10
0
100ms
Family 2
clutch
Bird 1
Bird 2
Bird 3
Family 3
clutch
Bird 1
Bird 2
Bird 3
Family 4
clutch
Bird 1
Bird 2

Figure I-4. Individual differences in stabilized song patterns in early-deafened zebra finches.

Zebra finches deafened at dph 18–22 developed unique song patterns with a characteristic motif-like structure (colored shadings) at the old adult stage (> dph 300). Sixteen early-deafened birds from four families are indicated.

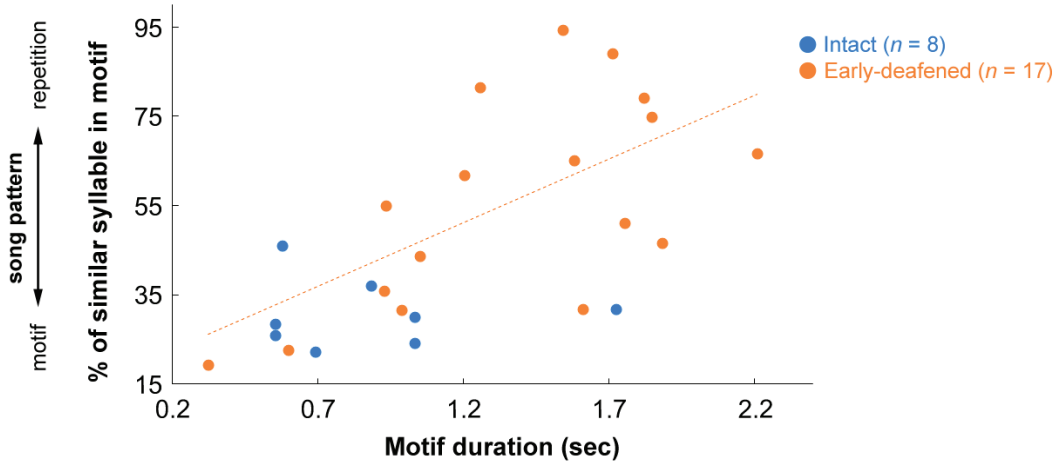
song pattern
repetition
motif
% of similar syllable in motif
95
75
55
35
15
0.2
0.7
1.2
1.7
2.2
Motif duration (sec)
Intact (n = 8)
Early-deafened (n = 17)

Figure I-5. Song of early-deafened birds possesses correlation between syllable similarity and motif duration.

Graph indicates relationship of syllable similarity in motif and motif duration at >dph 300. Each dot represents individual bird. Blue dots indicate intact (n = 8) and orange indicate early-deafened birds (n = 17). Using 60-100 syllables in a bird, similarity was calculated. % of high similarity (> 0.6 of similarity score) of syllable in all comparisons was then calculated to investigate how much syllables differentiate in a bird. Lower % of high similarity of syllable in motif means typical motif song pattern with several different syllables. Higher % means repetitive song pattern with one type syllables. Orange broken line represents approximate line of early-deafened birds. % of over 0.6 syllable similarity in motif is positively correlated with motif duration ($r = 0.63$, $p < 0.005$).

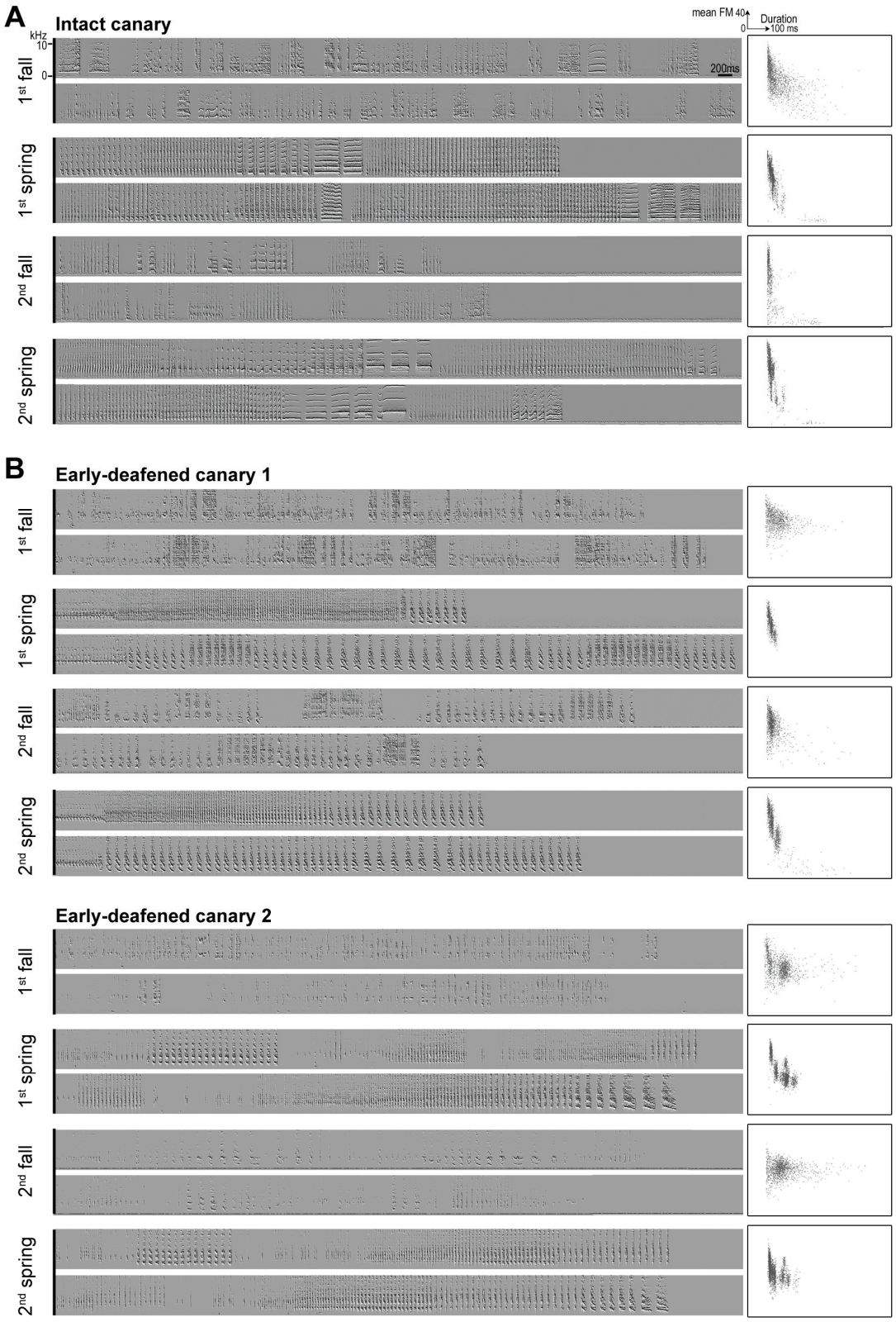
A
Intact canary
mean FM 40
0
Duration
100 ms
kHz
10
0
200ms
1st fall
1st spring
2nd fall
2nd spring
B
Early-deafened canary 1
1st fall
1st spring
2nd fall
2nd spring
Early-deafened canary 2
1st fall
1st spring
2nd fall
2nd spring

Figure I-6. Comparison of song development and stabilization between the intact and early-deafened canary.

***A*,** Example of song development and syllable scatter plots (duration versus mean FM) in an intact canary.

***B*,** Examples of song development and syllable scatter plots (duration versus mean FM) in two early-deafened canaries. The early-deafened canaries produced stabilized song in similar time course to those of the intact canary.

Chapter II

Activity of the Song Circuit during Audition-Independent Song Crystallization/Stabilization

2.1 Introduction

Songbirds and humans learn vocalization through tutor mimicry by auditory feedback. The learning of the birdsong, a complex sequenced motor pattern, occurs within a critical period during which the juvenile songbirds listen, memorize, and gradually match their own developing vocalizations to the song of the adult tutor.

Song production and learning are controlled by a network of interconnected brain areas called “song circuit” composed of two main pathways: 1) the vocal motor circuit containing HVC and the robustnucleus of the arcopallium (RA) that is critical for song production (Nottebohm et al., 1976; Simpson and Vicario, 1990) and 2) the basal ganglia–forebrain circuit anterior forebrain pathway (AFP) forming a loop from the lateral magnocellular nucleus (LMAN) in the pallium, through the Area X in the striatum and the dorsal lateral nucleus of the dorsomedial thalamus (DLM). AFP is necessary for generating vocal variability with direct premotor bias in response to vocal experience (Bottjer et al., 1984; Scharff and Nottebohm, 1991; Kao et al., 2005; Andalman and Fee, 2009).

I found that even without sensorimotor coordination through auditory feedback, the early-deafened zebra finches finally stabilized a vocal pattern; however, the timing of song crystallization was excessively delayed in comparison with that in intact birds (Chapter I). To elucidate where auditory deprivation affects the neural circuits that mediate vocal learning and production and how it causes delayed song development and audition-independent song crystallization, I compared the neural activity of the song nuclei using molecular mapping analysis of activity-induced genes (Jones et al., 2001; Wada et al., 2006; Horita et al., 2012) during singing between intact and early-deafened zebra finches.

First, I focused on the basal ganglia–forebrain circuit AFP which is considered to contribute to the vocal variability necessary for audition-dependent song plasticity (Kao et al.,

2005; Ölveczky, 2005; Andalman and Fee, 2009). Lesions of the AFP output nucleus, lateral magnocellular nucleus of the anterior nidopallium (LMAN), and basal ganglia nuclei Area X prevent song deterioration induced by auditory deprivation in the adult stage (Brainard and Doupe, 2000; Kojima et al., 2013). In addition, the pharmacological inactivation of LMAN dramatically reduces the acoustic and sequence variability of songs in the juvenile stage (Ölveczky, 2005). Based on these observations, I hypothesized that abnormally increased or decreased activity in the AFP nuclei during song development delays song development and stabilization in early-deafened birds. Nevertheless neural activity-dependent gene induction in song nuclei and the vocal output driven by the anterior basal ganglia–forebrain circuit were similar throughout development in both intact and deafened birds.

Following this, I examined the induction level of *Egr1* (*Zenk*), a neural activity-induced and neural plasticity-related gene (Jones et al., 2001), which was previously shown to be more highly induced by singing in the motor nucleus RA of juveniles than in that of adult birds (Jin and Clayton, 1997b). I hypothesized that auditory deprivation delays the developmental change in the induction level of *Egr1*and causes slower song stabilization in early-deafened birds. However, the *Egr1* expression dynamics in the motor circuit were similar between intact and early-deafened birds.

These results suggest that hearing loss did not affect the neural activity in the basal ganglia–forebrain circuit or in the vocal motor circuit. It has been reported that AFP biases the motor output to improve the match between auditory feedback and the tutor song (Andalman and Fee, 2009). When a bird is unable to acquire tutor song and use auditory feedback because of auditory deprivation, does AFP bias the vocal output? To examine whether the AFP-dependent bias contributes to generate the vocal pattern in early-deafened birds, I analyzed the songs of early-deafened birds with bilateral lesions of LMAN. I found that the

early-deafened birds are unable to develop a motif-like vocal pattern without LMAN. This result suggests that AFP innately possesses the bias to guide the species-specific structure.

2.2 Materials and Methods

Animals

I used male zebra finches from our breeding colony ranging from 47 to 1780 days post-hatching (dph). The photoperiod was constantly maintained at a 14:10 h light/dark cycle with food and water provided *ad libitum*. The sex of birds was checked by PCR as previously reported (Wada et al., 2006) within three days after hatching. The birds were raised in individual breeding cages with their parents and siblings until at least dph 30 and were then housed in single-sex groups (6–10 birds per cage) with visual and auditory access to both the male and female birds. I divided the animals into the following developmental stages to examine age-associated changes: dph 47–65 (juvenile), dph 100–187 (young adult), and >dph 300 (older adult). All animal experiments were performed according to the guidelines of the Committee on Animal Experiments of Hokkaido University from whom permission for this study was obtained. The guidelines are based on national regulations for animal welfare in Japan (Law for the Humane Treatment and Management of Animals; after partial amendment No.68, 2005).

Song recording and analysis

The birds were individually housed in sound-attenuation boxes (box size: 65 × 27 × 30 cm; cage size: 54 × 22 × 23 cm). Songs were automatically saved 24 h per day using the Sound Analysis Pro program (v1.04) (Tchernichovski et al., 2000) at 16 bits and a 44 kHz sampling rate. Analysis of syllable acoustic structure was performed using Sound Analysis Pro and Avisoft Saslab (Avisoft Bioacoustics). Low- and high-frequency noises (<0.5 kHz and >1.9 kHz) were filtered from the recordings using Avisoft Saslab, and the low frequency noises (<1.5 kHz) were further filtered using Sound Analysis Pro. For all analyses, I randomly selected songs per time-point and manually eliminated calls and cage noise from the dataset. The entropy and

amplitude parameters of syllables were set manually, and the syllables were segmented using Sound Analysis Pro. A song bout was defined as the continuous production of syllables followed by at least 400 ms of silence. Typical song bouts in adult zebra finches start with introductory notes followed by one or more motifs that consist of the same stereotyped sequence of syllables.

To examine correlation between amount of singing and expression level of immediate early genes as neural activity-dependent gene markers, I measured total singing duration (time spent producing songs) before brain sampling. I counted the number of bouts of singing within a day at least one day after the bird (either intact or deafened) was put into a sound-attenuated box (20 juveniles, n = 10/group; 19 young adults, n = 9–10/group; 21 older adults, n = 10–11/group).

Deafening

The birds were deafened by cochlear extirpation between dph 17–23 (before fledging) to establish the early-deafened group. The birds were anesthetized with pentobarbital (6.48 mg/ml; 60 μL/10 g of body weight) by intra peritoneal injection. After fixing the head in a custom-made stereotaxic apparatus with ear bars, a small window was made through the neck muscle and the skull near the end of the elastic extension of the hyoid bone. A small hole was then made in the cochlear dome. The cochlea was pulled out with a fine hooked wire. The removed cochleae were confirmed by visual inspection under a dissecting microscope. After bilateral cochlear removal, the birds were put back in their nest and kept with their parents and siblings until dph 32–41.

Brain lesion and its evaluation

I used 16 adult male birds for HVC lesion experiments (intact: n = 8; early-deafened: n = 8) and 4 early-deafened birds for LMAN lesion experiments. Songs recorded at least 2 days

before surgery. An early-deafened bird for LMAN lesion didn't sing before surgery. The bilateral HVC was lesioned by local injection of 0.44 μL 1% ibotenic acid dissolved in 1 M NaCl using a Nanoject 2 injector (Drummond Scientific). The bilateral LMAN was lesioned using combination of electrolytic lesions (up to 12 points) and injection of mineral oil to trace for long term development, over a year. Songs were then re-recorded multiple times after surgery. To examine the effect of HVC lesions on singing, syllable duration distributions were calculated using 700 syllables.

To confirm lesioned HVC size, the anesthetized birds were perfused with 1× PBS and then 4% paraformaldehyde/1× PBS. Sagittal sections, 30-μm thick, were cut on a freezing microtome and were free-floated in 1× PBS. The brain sections were then transferred to 0.3% H_2O_2/1× PBS for peroxidase inactivation, washed three times with 1× PBS, and reacted overnight at 4°C in blocking solution containing mouse anti-NeuN monoclonal antibody (1:2000; MILLIPORE). After three washes with 1× PBS, the sections were incubated in biotinylated goat anti-mouse IgG serum (1:400; Vector Laboratories), washed three times with 1× PBS, and then submerged in avidin–biotin–peroxidase complex solution (PK-6101, Vector Laboratories). Antibody labeling was visualized with DAB solution (SK4100, Vector Laboratories). I stained one of every four sections to estimate lesion size and location. LMAN lesions were examined by two measures, i.e. Nissl staining and *androgen receptor (AR)* expression, when the birds were over a year of age. A previous study has confirmed *AR* mRNA expression in LMAN of adult male. To perform these measures, I kept the birds alone in the sound-attenuation boxes overnight for silence, collected brain samples and conducted *in situ* hybridization with AR following a procedure described below.

Brain tissue collection

I collected brain samples to examine singing-related activity of song nuclei from the intact and early-deafened zebra finches under the following two conditions: (i) silence and darkness with no singing and just before switching the light on (intact: $n = 20$; early-deafened: $n = 19$) and (ii) with singing for 30–60 min after switching the light on (intact: $n = 19$; early-deafened: $n = 18$). To ensure similar circadian rhythms between the silent and singing conditions, sample collection was performed in the morning. In order to collect brain sample after singing, all the animals were individually placed in a sound-attenuated box at least 2 days prior to singing, and they were subsequently sacrifice by decapitation. In both groups, the brains were rapidly removed, frozen in a plastic mold with Tissue-Tek OCT compound (Sakura Fine Technical) placed on dry ice, and stored at −80°C until use for *in situ* hybridization.

Radioisotopic in situ hybridization and quantification

Serial sagittal sections, 12 μm thick, were cut throughout the brain and ^{35}S-labeled riboprobe *in situ* hybridization was performed as described (Wada et al., 2004). I first amplified cDNA fragments [*Dusp1*, *Egr1* and *AR*] by PCR from the zebra finch whole-brain first-strand cDNA and cloned them into pGEMT-easy vectors. PCR was performed to amplify the plasmid region that included the cloned cDNA between T7 and SP6 RNA polymerase binding regions. The resulting PCR fragment was used as the DNA template for T7 or SP6-primed *in vitro* transcription to synthesize ^{35}S-labeled riboprobes for *in situ* hybridization. Frozen sections were fixed in 3% paraformaldehyde/1× PBS, acetylated, dehydrated in an ascending ethanol series, and then hybridized with ^{35}S-labeled riboprobe (1×10^6 cpm/slide) in hybridization solution [50% formamide, 10% dextran, 1× Denhardt's solution, 12 mM EDTA, 10 mM Tris HCL (pH 8.0), 30 mM NaCl, 0.5 μg/μL yeast tRNA, 10 mM DTT] at 65°C for 14 h. The slides were then

washed and exposed to β-Max Hyperfilm (Kodak) before being immersed in NTB-2 emulsion (Kodak) for 2–5 weeks. The slides were then developed and stained with cresyl violet. The signal intensity of mRNAs in song nuclei and other brain regions was calculated by a previously described procedure (Wada et al., 2006). The exposed X-ray films of brain images were digitally scanned under a dissecting microscope (Z16 APO, Leica) connected to a CCD camera (DFC490, Leica) using Application Suite V3 imaging software (Leica). The same light and camera settings were used for all images to facilitate comparison. I used Photoshop (Adobe Systems) to measure the mean pixel intensities in the brain areas of interest from two or more adjacent sections after conversion to a 256 gray scale.

I performed regression analysis using the statistical software R (http://www.r-project.org/; R Core Team, 2013; R Foundation for Statistical Computing) to compare *Dusp1* and *Egr1* expression levels induced by singing in the AFP between the six experimental groups.

2.3 Results

2.2.1 Neural activity in song nuclei during singing

I set out to examine where and how auditory deprivation affects the neural circuits that mediate vocal learning and production and causes delayed song development and audition-independent song crystallization.

First, I hypothesized that different rates of song development between the intact and deafened birds reflect differences in AFP activity during development. To test the possibilities, I compared the neural activity of AFP among juvenile (dph 47–59, mean ± SEM; dph 55.17 ± 0.58), young adult (dph 102–147, mean ± SEM; dph 133.16 ± 3.89), and older adult (dph 327–1715, mean ± SEM; dph 881.06 ± 67.24) birds (both intact and early-deafened) using two approaches, molecular mapping analysis of activity-induced genes (Wada et al., 2006; Horita et al., 2012) and behavioral analysis of vocal outputs driven by AFP (Aronov et al., 2008). The neural activity-induced genes dual-specific phosphatase 1 (*Dusp1*) and *c-fos* were used as molecular markers of AFP activity because both are induced by singing in all three AFP song nuclei: LMAN, striatum nucleus Area X, and dorsal lateral nucleus of the medial thalamus (DLM) (**Fig. II-1**). There were no significant differences in singing-induced expression levels of *Dusp1* in the same nuclei between age-matched early-deafened and intact birds (**Fig. II-2**). The consistent result was also observed with the *c-fos* probe (**Fig. II-3**). Furthermore, after bilateral lesions of the premotor nucleus HVC, both the intact and early-deafened birds at young and adult stages exhibited highly similar AFP-driven vocal outputs with coincident syllable duration distributions (**Fig. II-4**). These results suggest that molecular signaling cascades in the AFP nuclei and AFP-driven premotor outputs are similarly regulated regardless of age or the presence of auditory inputs.

Next, I measured the induction level of *Egr1*, a neural activity-induced and neural

plasticity-related gene (Jones et al., 2001) to examine whether auditory deprivation affects the developmental change of gene induction level in the vocal motor circuit. As previously reported, *Egr1* expression in the RA was significantly higher after singing during the juvenile plastic song phase (dph 47–59) than that during young adult (dph 104–147) or older adult (dph 327–1715) crystallized-song phases in the intact birds (regression analysis, $p < 0.05$, **Fig. II-5**). In addition, in the early-deafened zebra finches, *Egr1* expression dynamics in the motor nuclei HVC and RA were very similar to the intact birds, although the intact and early-deafened birds developed individual song patterns at different rates (**Fig. II-5**), suggesting that expression of neural plasticity-related genes during development is not substantially altered by auditory input.

2.2.2 Role of activity of the basal ganglia-forebrain circuit in generating audition-independent vocal pattern

The above results indicate unaltered activity of the AFP and motor circuit throughout song development in both the intact and deafened birds. The basal ganglia–forebrain circuit AFP is involved in generating an error-reducing bias, which improves performance in the motor circuit depending on auditory feedback (Andalman and Fee, 2009). Based on these facts, there is the possibility, in early-deafened birds, the basal ganglia-forebrain circuit could generate vocal variability but without the bias because of the hearing loss. To examine whether the input from the AFP to the motor circuit involved in generating audition-independent vocal pattern or not, I performed bilateral lesions of LMAN, the nucleus of output of the AFP, to the early-deafened bird during subsong stage (dph 41-46). The early-deafened birds with LMAN lesions produced repetitive and long duration song at over dph 300, in contrast to song of LMAN intact and early-deafened birds varied from motif like song to repetitive song (**Fig. II-6**). Although this is the data from limited numbers of birds and additional experiment is needed,

this result suggests that the basal ganglia-forebrain circuit involves in generating song pattern, like motif structure, independently of audition in zebra finch.

2.4 Discussion

The birdsong, like human speech, results from the development of specialized brain regions for vocal learning and production. However, how the auditory input affects neural activity in the song nuclei is not well understood. I found that the gene induction levels of neural activity-dependent genes and the vocal output driven by AFP were similar throughout development in both intact and deafened birds. During the critical period, singing-driven gene expression of *Dusp1*, *c-fos*, and *Egr1* was unaltered in the absence of audition an input in both AFP and motor circuits, even in the case of long-term auditory deprivation.

A large set of neural plasticity-related genes in song nuclei are regulated by singing (Li et al., 2000; Poopatanapong et al., 2006; Wada et al., 2006), which suggests that singing-driven gene expression is also regulated purely by motor activity and not sensory information (hearing input) (Teramitsu et al., 2010). Therefore, volitional singing itself (and/or total amount of singing) as a motor activity could be a crucial developmental epigenetic factor that activates the genetic programs to regulate vocal plasticity and develop species-specific vocal patterns, just as the potency of the external environment provides experience-dependent stimulation that regulates the critical periods and neural plasticity of sensory-related circuits (Hensch, 2004; Knudsen, 2004). Recently, it was shown that both neural plasticity-related genes and epigenetic regulators are induced by neural activity. The direct epigenetic regulators, a DNA demethylation regulator *Gadd45b* (Ma et al., 2009) and a replacement histone *H3.3b* (Michod et al., 2012), are induced by singing-driven neural activation in song nuclei in both intact and deafened birds (Wada et al., 2006; unpublished data). Although the data indicating direct relationships between motor-driven epigenetic regulation and developmentally regulated gene expression dynamics are still limited, neural activity-dependent modification of the DNA methylation landscape and subsequent gene expression changes have been demonstrated in the adult brain (Guo et al.,

2011b; Guo et al., 2011a). Therefore, audition-independent genetic programs in the song system may be directly or indirectly regulated by activation of the singing (motor)-dependent epigenetic factors. This idea fits with the observation that the intact and early-deafened birds exhibited a similar amount of singing during development (**Fig. I-4*B***), which can be examined by an experiment that includes long-term singing inhibition during the critical period of vocal learning, which might determine whether singing-inhibited songbirds showed delayed gene expression dynamics in song circuits.

How do early-deafened birds develop their songs and finally crystallize song patterns without a tutor song and their vocal feedback information? Even though collateral afferent feedback from the syrinx and/or respiratory organs may guide neural maturation and song formation in a deafened condition, the AFP has been considered to generate the vocal exploration necessary for audition-dependent song learning to match with a tutor song (Andalman and Fee, 2009; Charlesworth et al., 2012). Therefore, it is speculated that the early-deafened birds continue random exploration of vocal outputs in their life. However, this supposed exploration of vocal outputs was not observed at the old adult stage even if the AFP is active while singing **(Fig. I-1, II-2, II-3**). Song development of the early-deafened birds is delayed, but their song patterns were eventually stabilized. Similarly, songbird pupils do not continue to generate variable vocal outputs until they match the tutor song. Instead, they generate unique song patterns as their crystallized songs when they mature (Tchernichovski and Nottebohm, 1998). These facts suggest the transfer of functional dominance from the AFP to the motor circuit is crucial for regulating vocal plasticity and stabilization, and this transference would persist under audition deprivation.

In addition, when the early-deafened birds had an LMAN lesion, I never observed that a motif-like structure appeared without the input from the basal ganglia–forebrain circuit to the

motor circuit, whereas the early-deafened birds developed a species-specific motif pattern. Hearing–intact birds that received bilateral ablation of LMAN at the juvenile stage also produce a repetitive song pattern consisting of only one or two syllables (Bottjer et al., 1984; Scharff and Nottebohm, 1991; Elliott et al., 2014). The basal ganglia–forebrain circuit is considered to play a role in shaping juvenile vocal behavior toward the acoustic structure of the tutor song by differentiating song syllables (Elliott et al., 2014). This suggests the possibility that the basal ganglia–forebrain circuit innately possesses the bias that differentiates the syllables toward the species-specific pattern, like a motif. These results indicate that the inherent end-point for song stabilization is regulated by audition- and AFP-independent ways, and further suggest the existence of intrinsic neural mechanisms for developing song phenotypes with species constraints and diversification.

2.5 Figures

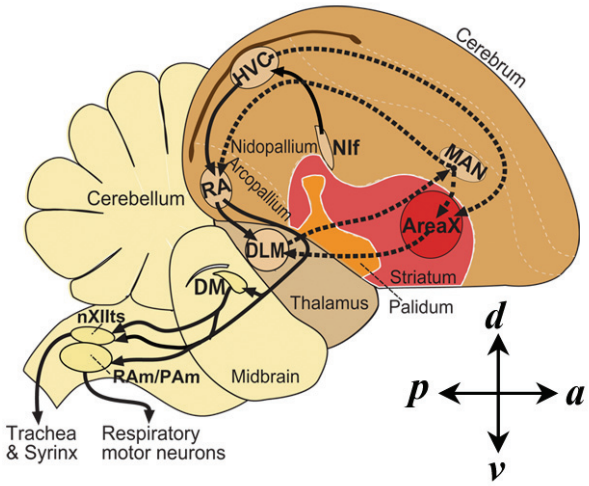
Cerebrum
HVC
Nidopallium
NIf
MAN
RA
Arcopallium
Cerebellum
Area X
DLM
Striatum
DM
Thalamus
Palidum
nXIIts
RAm/PAm
Midbrain
Trachea
& Syrinx
Respiratory
motor neurons
d
p
a
v

Figure II-1. Diagram of brain song circuits.

Drawing illustrates a brain section from a male zebra finch. Black solid lines denote connections within the posterior vocal motor circuit and black dashed lines within the basal ganglia–forebrain circuit AFP. HVC: a vocal nucleus (no acronym), RA: robust nucleus of the arcopallium, DM: dorsal medial nucleus of the midbrain, DLM: dorsal lateral medial nucleus of the thalamus, MAN: magnocellular nucleus of the anterior nidopallium, LMAN: lateral MAN, Area X: a vocal nucleus (no acronym), nXIIts: twelfth nucleus, tracheosyringeal part, Ram/Pam: nucleus retroambiguus/parambiguus.

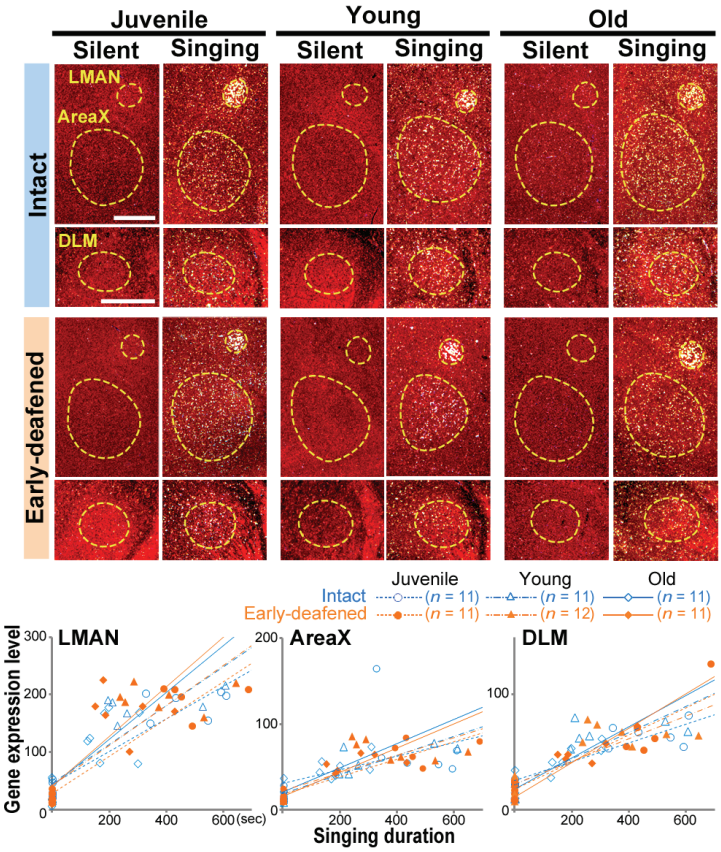
Juvenile
Young
Old
Silent
Singing
LMAN
AreaX
DLM
Intact
Early-deafened
Juvenile
Young
Old
Intact (n = 11) (n = 11) (n = 11)
Early-deafened (n = 11) (n = 12) (n = 11)
LMAN
AreaX
DLM
Gene expression level
Singing duration
(sec)

Figure II-2. Similar induction of neural activity-induced gene expression from the basal ganglia–forebrain circuit (AFP) pre- and post-song crystallization/ stabilization.

Singing-driven *Dusp1* mRNA expression in the AFP song nuclei, LMAN, Area X, and DLM in intact and early-deafened zebra finches at juvenile (dph 47–59), young (dph 102–147), and old (dph 327–1715) stages. The young stage is pre-song stabilization stage for early-deafened finches and post-stabilization for intact finches. The old stage is post-stabilization for early-deafened finches. White and red represent the *Dusp1* mRNA signal and Nissl counter-stained cells, respectively, in sagittal brain section (right: anterior, up: dorsal). Scale bar = 1 mm. Summarized graphs show the relationship between total singing duration and *Dusp1* gene expression level in LMAN, Area X, and DLM. There is little difference in this relationship between intact and early-deafened songbirds at all three developmental stages (LMAN: $p = 0.83$; Area X: $p = 0.36$; DLM: $p = 0.11$; regression analysis). Each dot represents individual values; the regression line is indicated for each group (intact: blue, early-deafened: orange; juveniles: circles, young adults: triangle, old adults: diamonds).

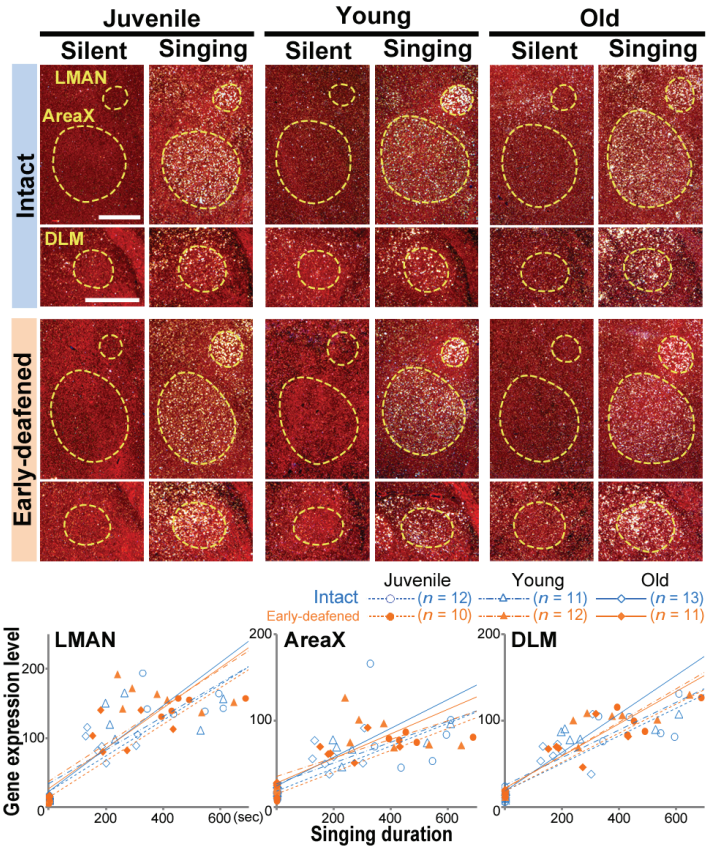
Juvenile
Young
Old
Silent
Singing
Silent
Singing
Silent
Singing
LMAN
AreaX
DLM
Intact
Early-deafened
Juvenile
Young
Old
Intact (n = 12) (n = 11) (n = 13)
Early-deafened (n = 10) (n = 12) (n = 11)
LMAN
AreaX
DLM
Gene expression level
200
100
0
200
400
600 (sec)
Singing duration

Figure II-3. Similar induction of *c-fos* expression in the basal ganglia–forebrain circuit (AFP) pre- and post-song crystallization/ stabilization.

Singing-driven *c-fos* mRNA expression in the AFP song nuclei, LMAN and Area X in intact and early-deafened zebra finches at juvenile (dph 47–59), young (dph 102–147), and old (dph 327–1715) stages. The young stage is pre-song stabilization stage for early-deafened finches and post-stabilization for intact finches. The old stage is post-stabilization for early-deafened finches. White and red represent the *c-fos* mRNA signal and Nissl counter-stained cells, respectively, in sagittal brain section (right: anterior, up: dorsal). Scale bar = 1 mm. Summarized graphs show the relationship between total singing duration and *c-fos* gene expression level in LMAN and Area X. There is little difference in this relationship between intact and early-deafened songbirds at all three developmental stages (LMAN: $p = 0.82$; Area X: $p = 0.37$; DLM: $p = 0.95$; regression analysis). Each dot represents individual values; the regression line is indicated for each group (intact: blue, early-deafened: orange; juveniles: circles, young adults: triangle, old adults: diamonds).

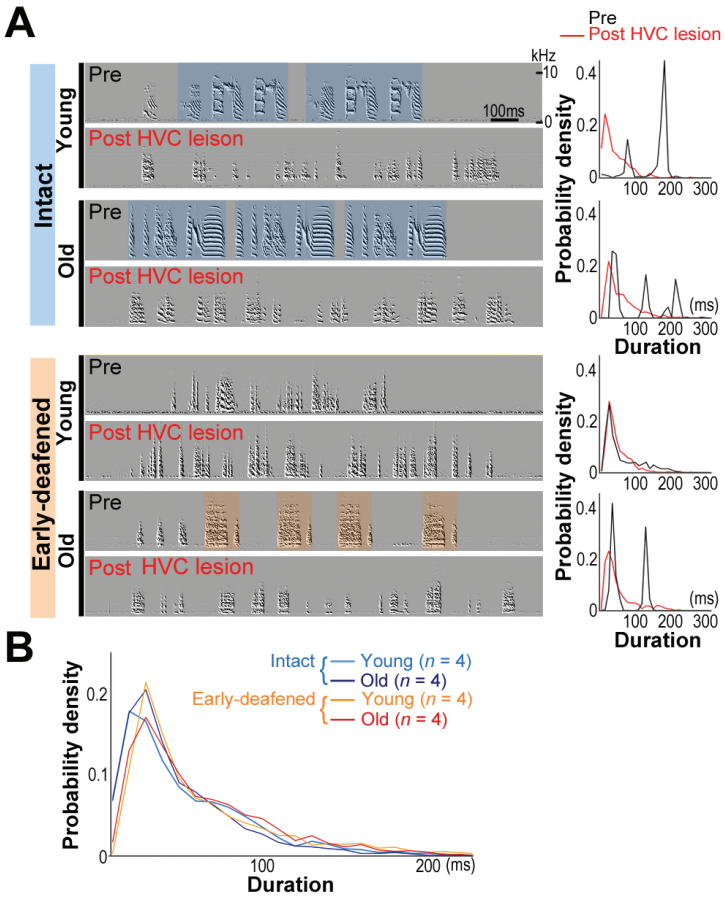
A
Pre
Post HVC lesion
kHz
10
0
100ms
Intact
Young
Old
Early-deafened
Pre
Post HVC leison
Post HVC lesion
Post HVC lesion
Probability density
0.4
0.2
0
100 200 300
(ms)
Duration
B
Intact
Young (n = 4)
Old (n = 4)
Early-deafened
Young (n = 4)
Old (n = 4)
Probability density
0.2
0.1
0
100
200 (ms)
Duration

Figure II-4. Similar vocal output from the basal ganglia–forebrain circuit (AFP) pre- and post-song crystallization/ stabilization.

***A*,** Example of similar vocal outputs following HVC lesion (producing AFP-driven songs) at young and old adult stages in both intact and early-deafened zebra finches. Characteristic motif-like structures are shaded. Changes in song patterns (left) and distributions of syllable durations (right) pre- and post-HVC lesion (black and red lines, respectively).

***B*,** Average probability density distribution of syllable duration for AFP-driven songs after HVC lesion (light blue: young intact bird at dph 115–138; blue: old intact bird at dph 660–1746; orange: young early-deafened songbird at dph 108–159; and red: old early-deafened songbird at dph 549–1037).

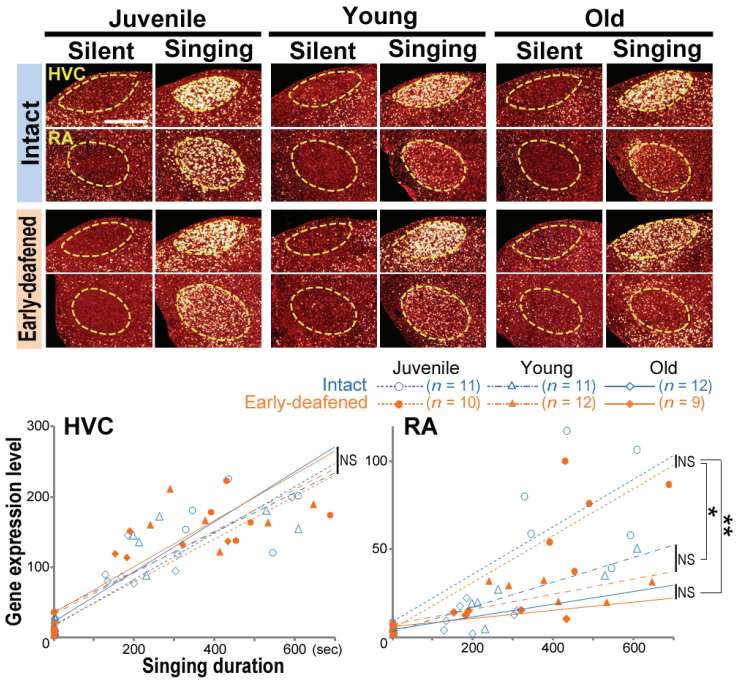
Juvenile
Young
Old
Silent
Singing
Silent
Singing
Silent
Singing
HVC
RA
Intact
Early-deafened
Juvenile
Young
Old
Intact (n = 11) (n = 11) (n = 12)
Early-deafened (n = 10) (n = 12) (n = 9)
HVC
RA
Gene expression level
Singing duration
(sec)
NS
NS
NS
NS
*
**

Figure II-5. Developmental regulation of singing-induced *Egr1* expression in the motor circuit among intact and early-deafened zebra finches.

In contrast to the HVC, induction of *Egr1* mRNA expression is differentially regulated through development in RA, i.e., higher in the juvenile (dph 47–59) than in the young (dph 102–147) and old adult (dph 327–1715) stages for both intact and early-deafened birds (HVC: $p = 0.55$; RA: $*p = 0.0232$ for juvenile versus young; $**p = 0.0017$ for juvenile versus old, regression analysis). However, there is no significant difference in the induction rate of *Egr1* among developmental stage-matched intact and early-deafened groups in HVC and RA (juvenile; $p = 0.6024$, young; $p = 0.7451$, old; $p = 0.8153$ for intact versus early-deafened birds in RA, regression analysis). Each dot represents individual values; the regression line is indicated for each group (intact: blue, early-deafened: orange; juveniles: circles, young adults: triangle, old adults: diamonds). White and red represent *Egr1* mRNA signal and Nissl counter-stained cells, respectively, in sagittal brain section (right: anterior, up: dorsal). Scale bar = 1 mm.

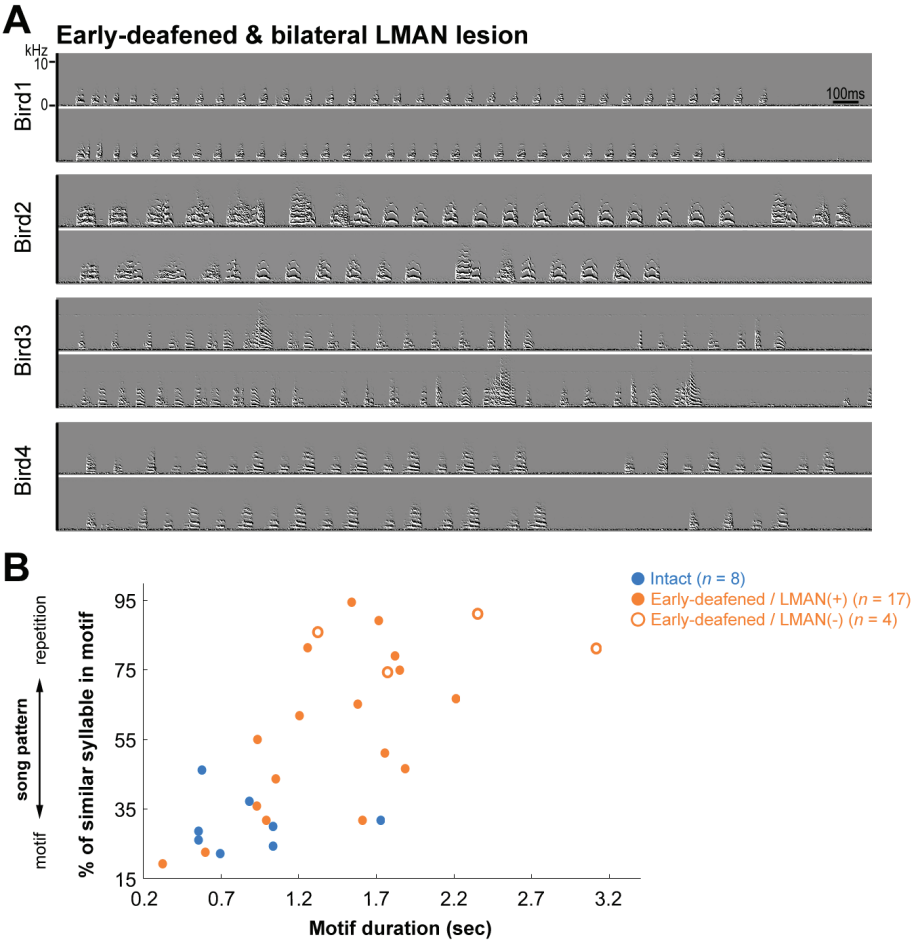
A
Early-deafened & bilateral LMAN lesion
kHz
10
0
100ms
Bird1
Bird2
Bird3
Bird4
B
Intact (n = 8)
Early-deafened / LMAN(+) (n = 17)
Early-deafened / LMAN(-) (n = 4)
song pattern
repetition
motif
% of similar syllable in motif
95
75
55
35
15
0.2
0.7
1.2
1.7
2.2
2.7
3.2
Motif duration (sec)

Figure II-6. Input from the basal ganglia-forebrain circuit to the motor circuit affect the development of vocal pattern in early-deafened birds.

A. Examples of song and syllable scatter plots (duration versus mean FM) at > dph300 in four early-deafened birds with bilateral LMAN lesion.

B. Graph indicates relationship of syllable similarity in motif and motif duration at >dph 300 as the same in **Fig. I-5**. Each dot represents individual bird. Blue dots indicate intact (n = 8), filled orange dots indicate early-deafened birds (n = 17), and open orange dots indicate early-deafened birds received bilateral LMAN lesion (n = 4). Using 60-100 syllables in a bird, similarity was calculated. % of high similarity (> 0.6 of similarity score) of syllable in all comparisons was then calculated to investigate how much syllables differentiate in a bird. Lower % of high similarity of syllable in motif means typical motif song pattern with several different syllables. Higher % means repetitive song pattern with one type syllables.

Chapter III

Audition-Dependent Sensitivity and Audition-Independent Robustness of Gene Expression Dynamics in the Motor Circuit during Song Development

3.1 Introduction

The birdsong is a complex learned vocalization that is developed through the coordination between a motor output and auditory feedback. This sensorimotor coordination aiming to imitate a memorized tutor song is one of the critical processes for vocal learning. However, the exact role of the auditory input in the neural circuit maturation for vocal learning and production is not well understood. Using audition-deprived songbirds, I examined whether auditory experience affects developmental gene expression in the song nuclei, representing major elements of neural circuits.

Because I observed unaltered AFP activity throughout song development in both intact and deafened birds (Chapter II), I considered the possibility that the autonomous changes associated with song development regulation and crystallization timing exist in the vocal motor output circuit. A decrease in vocal variability has been attributed to the strengthening of inputs from HVC and the concurrent weakening of inputs from LMAN to RA at the synaptic level (Herrmann and Arnold, 1991; Stark and Perkel, 1999). Furthermore, HVC is the only song system nucleus that receives direct projections from auditory areas (Bauer et al., 2008). Adult deafening reduces the size of dendritic spines and alters spontaneous action potential activity in HVC projection neurons to Area X (Tschida and Mooney, 2012). Therefore, HVC and RA might be affected by audition deprivation and delayed vocal development. In addition, several studies have indicated a relationship between song development and gene expression changes in the motor circuit (Soderstrom and Tian, 2006; Wada et al., 2006; Balmer et al., 2009; Matsunaga et al., 2011).

I conducted global transcriptome analysis in both intact and early-deafened zebra finches because acquisition of complex song pattern should be achieved by orchestral contribution of a large variety of genes, and not by a few restricted numbers of genes. Compared with intact zebra

finches, early-deafened zebra finches showed excessively delayed vocal development, but their songs eventually crystallized (Chapter I). In contrast to the different rates of song development between the intact and deafened birds, developmental gene expression in the motor circuit is conserved in an age-dependent manner from the juvenile stage until the older adult stage, even in the deafened birds, which indicates the audition-independent robustness of gene expression dynamics during development. Further, even after adult deafening, which degrades crystallized song, the deteriorated songs ultimately re-stabilized at the same point when the early-deafened birds stabilized their songs. These results indicate a genetic program-associated inevitable termination of vocal plasticity that results in audition-independent vocal crystallization.

3.2 Materials and Methods

Animals

I used male zebra finches from our breeding colony ranging from 47 to 1327 days post-hatching (dph). The photoperiod was constantly maintained at a 14:10 h light/dark cycle with food and water provided *ad libitum*. The sex of birds was checked by PCR as previously reported (Wada et al., 2006) within three days after hatching. The birds were raised in individual breeding cages with their parents and siblings until at least dph 30 and were then housed in single-sex groups (6–10 birds per cage) with visual and auditory access to both the male and female birds. I divided the animals into the following developmental stages to examine age-associated changes: dph 47–65 (juvenile), dph 100–187 (young adult), and >dph 300 (older adult). All animal experiments were performed according to the guidelines of the Committee on Animal Experiments of Hokkaido University from whom permission for this study was obtained. The guidelines are based on national regulations for animal welfare in Japan (Law for the Humane Treatment and Management of Animals; after partial amendment No.68, 2005).

Song recording and analysis

The birds were individually housed in sound-attenuation boxes (box size: 65 × 27 × 30 cm; cage size: 54 × 22 × 23 cm). Songs were automatically saved 24 h per day using the Sound Analysis Pro program (v1.04) (Tchernichovski et al., 2000) at 16 bits and a 44 kHz sampling rate. Analysis of syllable acoustic structure was performed using Sound Analysis Pro and Avisoft Saslab (Avisoft Bioacoustics). Low- and high-frequency noises (<0.5 kHz and >1.9 kHz) were filtered from the recordings using Avisoft Saslab, and the low frequency noises (<1.5 kHz) were further filtered using Sound Analysis Pro. For all analyses, I randomly selected songs per time-point and manually eliminated calls and cage noise from the dataset. The entropy and

amplitude parameters of syllables were set manually, and the syllables were segmented using Sound Analysis Pro. A song bout was defined as the continuous production of syllables followed by at least 400 ms of silence. Typical song bouts in adult zebra finches start with introductory notes followed by one or more motifs that consist of the same stereotyped sequence of syllables.

To examine correlation between amount of singing and expression level of immediate early genes as neural activity-dependent gene markers, I measured total singing duration (time spent producing songs) before brain sampling. I counted the number of bouts of singing within a day at least one day after the bird (either intact or deafened) was put into a sound-attenuated box (20 juveniles, n = 10/group; 19 young adults, n = 9–10/group; 21 older adults, n = 10–11/group).

To compute correlations between song traits and DNA microarray expression data, I calculated mean values and coefficients of variation (CV) of nine song parameters: (i) syllable duration, (ii) amplitude, (iii) pitch, (iv) frequency modulation (FM), (v) Wiener entropy, (vi) goodness of pitch, (vii) inter syllable duration, (viii) syllable number in a motif, and (ix) motif consistency, for each bird from 100 syllables recorded within a week before brain sampling. Motif consistency was measured as motif similarity score within a day and was calculated by the default setting in the Sound Analysis Pro software using the “time-course” and “symmetric” comparison modes. This procedure can calculate the similarity score between two motifs on the basis of comparison of syllable acoustic features (*e.g.*, pitch, FM, AM, Wiener entropy, and goodness of pitch) within sliding 9-ms time windows and represents a global measure of percent similarity. For motif consistency analysis, song motifs were extracted from sequences of 3–5 syllables at the beginning of the bout but excluding introductory notes. I compared 20 randomly selected motifs in each bird.

Deafening

The birds were deafened by cochlear extirpation between dph 17–23 (before fledging) to establish the early-deafened group or at dph 92–157 (after song crystallization) to establish the adult deafened group. The birds were anesthetized with pentobarbital (6.48 mg/ml; 60 μL/10 g of body weight) by intra peritoneal injection. After fixing the head in a custom-made stereotaxic apparatus with ear bars, a small window was made through the neck muscle and the skull near the end of the elastic extension of the hyoid bone. A small hole was then made in the cochlear dome. The cochlea was pulled out with a fine hooked wire. The removed cochleae were confirmed by visual inspection under a dissecting microscope. After bilateral cochlear removal, the birds were put back in their nest and kept with their parents and siblings until dph 32–41.

Brain tissue collection

I collected brain samples from the intact and early-deafened zebra finches under the following two conditions: (i) silence and darkness with no singing and just before switching the light on (intact: n = 17; early-deafened: n = 18; adult-deafened: n = 5) and (ii) with singing for 30–60 min after switching the light on (adult-deafened: n = 6). To ensure similar circadian rhythms between the silent and singing conditions, sample collection was performed in the morning. In order to collect brain sample after singing, all the animals were individually placed in a sound-attenuated box at least 2 days prior to singing, and they were subsequently sacrifice by decapitation. In both groups, the brains were rapidly removed, frozen in a plastic mold with Tissue-Tek OCT compound (Sakura Fine Technical) placed on dry ice, and stored at −80°C until use for *in situ* hybridization or for laser capture microdissection (LCM).

Radioisotopic in situ hybridization and quantification

Serial sagittal sections, 12-μm thick, were cut throughout the brain and ^{35}S-labeled riboprobe *in situ* hybridization was performed as described (Wada et al., 2004). I first amplified cDNA fragments [hairy/enhancer-of-split related with YRPW motif protein 1 (*Hey1*), MAX-interacting protein 1 (*Mxi1*), neuronal differentiation 6 (*Neurod6*), sex determining region Y-box 4 (*Sox4*), and zinc finger protein 238 (*Znf238*)] by PCR from the zebra finch whole-brain first-strand cDNA, and cloned them into pGEMT-easy vectors. PCR was performed to amplify the plasmid region that includes the cloned cDNA between T7 and SP6 RNA polymerase binding regions. The resulting PCR fragment was used as the DNA template for T7 or SP6-primed *in vitro* transcription to synthesize ^{35}S-labeled riboprobes for *in situ* hybridization. Frozen sections were fixed in 3% paraformaldehyde/1× PBS, acetylated, dehydrated in an ascending ethanol series, and then hybridized with ^{35}S-labeled riboprobe (1×10^6 cpm/slide) in hybridization solution [50% formamide, 10% dextran, 1× Denhardt's solution, 12 mM EDTA, 10 mM Tris HCL (pH 8.0), 30 mM NaCl, 0.5 μg/μL yeast tRNA, 10 mM DTT] at 65°C for 14 h. The slides were then washed and exposed to β-Max Hyperfilm (Kodak) before being immersed in NTB-2 emulsion (Kodak) for 2–5 weeks. The slides were then developed and stained with cresyl violet. The signal intensity of mRNAs in song nuclei and other brain regions was calculated by a previously described procedure (Wada et al., 2006). The exposed X-ray films of brain images were digitally scanned under a dissecting microscope (Z16 APO, Leica) connected to a CCD camera (DFC490, Leica) using Application Suite V3 imaging software (Leica). The same light and camera settings were used for all images to facilitate comparison. I used Photoshop (Adobe Systems) to measure the mean pixel intensities in the brain areas of interest from two or more adjacent sections after conversion to a 256 gray scale.

I performed regression analysis using the statistical software R

(http://www.r-project.org/; R Core Team, 2013; R Foundation for Statistical Computing) to compare expression levels of *Hey1*, *Mxi1*, *Neurod6*, *Sox4*, and *Znf238*, *F*-tests were first performed to confirm the homoscedasticity of the expression ratio between song nuclei, followed by Student's *t* tests or Welch's *t* tests. For all tests, statistical significance was considered at $p < 0.05$ after Bonferroni correction.

Laser capture microdissection (LCM)

The brains were serially cryosectioned at 14-μm thick onto handmade membrane slides for LCM. The tissue sections were stained for Nissl bodies to histologically confirm the presence and boundaries of each nucleus and were then dehydrated prior to LCM. Briefly, frozen sections were sequentially exposed to 75% EtOH for 30 s, 50% EtOH for 30 s, cresyl violet for 15 s, 50% EtOH for 30 s, 75% EtOH for 30 s, 95% EtOH for 30 s, 100% EtOH for 30 s, 100% EtOH for 1 min, 100% EtOH for 3 min, 2 × 2 min xylene, and finally air dried for 5 min (LCM Staining kit, Ambion). HVC and RA tissues were microdissected using a laser capture microscope (ArcturusXT^{TM}, Arcturus Bioscience). The laser parameters for LCM were as follows: spot diameter 100 μm, laser power 80 mW, and laser duration 80 ms. The microdissected tissue was directly collected into RLT Buffer from the RNeasy Micro kit (QIAGEN) supplemented with β-mercaptoethanol. The samples were vortexed, centrifuged, and stored at −80°C until RNA purification.

RNA purification, amplification, and confirmation of the linearity of amplification

I isolated and amplified RNA according to the procedures of the Agilent Gene Expression FFPE Workflow (http://www.chem.agilent.com/Library/applications/5990-3917en_hi.pdf). RNA was column-purified (RNeasy Micro kit, QIAGEN) and treated with DNase on the

column to remove genomic DNA. To quantify RNA quality, RNA integrity number (RIN) and concentration were measured by a Bioanalyzer 2100 (Agilent Technologies). Because of the limited yield of extracted RNA, I randomly selected four RNA samples to examine RIN and RNA concentration (RIN: 5.9–7.1; RNA concentration: 1.69–2.35 ng/μL) Purified RNA was amplified using the TransPlex Whole Transcriptome Amplification kit (WTA2 kit, Sigma–Aldrich) according to the manufacturer's instructions. The amplified cDNA was purified by removal of residual primers and nucleotides using the QIAquick PCR purification kit (QIAGEN). Quality and yield of the amplified cDNA were measured by a NanoDrop ND-8000 (Thermo Scientific) and by electrophoresis. A 1.7 μg sample of total amplified cDNA was converted into Cy3-labeled cDNA using the Genomic DNA ULS labeling kit (Agilent Technologies) following the Agilent Gene Expression FFPE Workflow. Labeled cDNAs from each sample were hybridized to a DNA microarray.

DNA microarrays

Agilent zebra finch 44k × 4 oligoarrays (AMADID No. 021323) containing 44,969 cDNA 60-mer probes (including 11,549 genes as gene-symbol identified genes) were designed at the Jarvis Laboratory of Duke University on the basis of sequence information of cDNA libraries from Duke University, Michigan State University, Rockefeller University, and the Keck Center of the University of Illinois (Wada et al., 2006; Li et al., 2007; Replogle et al., 2008). HVC and RA tissue samples (each n = 3 at juvenile, young, and old stages) were laser-microdissected from the intact and early-deafened birds (for both the intact and early-deafened birds at juvenile, young, and old stages: n = 4, 5, and 3 birds, respectively). Because of experimental difficulty at the RNA amplification step, some birds were used for only HVC or RA (thus, the number of sample birds at some stages exceeded 3). Single-channel

hybridizations were conducted for each sample that was hybridized to a single array. Because four arrays were separately printed on a slide, I hybridized four samples matched for the age and brain region as a single batch to minimize possible inter-slide bias or batch effects. After hybridization, the arrays were washed and scanned, and the data was extracted from the scanned images (G2505B, Agilent Technologies) using Feature Extraction version 9.1 (Agilent Technologies). The DNA microarray data reported in this study was deposited in the Gene Expression Omnibus (GEO) database (accession no. GSE56075).

DNA microarray statistical analysis

All subsequent preprocessing and analyses were performed using Microsoft Excel and the statistical software R. Probe refers to a single probe on the array. For the majority of gene-symbol identified genes, multiple probes were present on the array. HVC and RA samples were separated, and the two datasets preprocessed separately as follows. First, control probes were removed and probes with raw fluorescence values >3 standard deviations (SD) from the mean of all samples for that probe were removed. To reduce noise, probes with raw fluorescence values <50 in more than 80% of samples in each nuclei were removed. A total of 41,525 probes for 11,391 gene-symbol identified genes in HVC and 41,340 probes for 11,374 gene-symbol identified genes in RA fit these criteria and were processed. Arrays were quantile normalized and the fluorescence value was transformed to $\log_2$ scale.

Analysis of variance (ANOVA) was used to identify probes differentially expressed between developmental stages in the intact birds ($p < 0.05$; 3,362 and 1,466 probes in HVC and RA, respectively). The expression levels of these genes were compared between the intact and early-deafened birds to assess how auditory input influenced gene expression levels. Principal component analysis (PCA) using the prcomp package and three-dimensional view using the rgl

package in R were used to visualize the separation of samples.

Weighted gene co-expression network analysis (WGCNA) was performed using the WGCNA R package for further investigation of the relation between biological traits (age, audition status, and song characteristics) and clusters of co-regulated genes (Langfelder and Horvath, 2008). General information about network analysis methodology and WGCNA software is available at http://labs.genetics.ucla.edu/horvath/htdocs/CoexpressionNetwork/. Differentially expressed probes (9,903 and 6,536 probes in HVC and RA, respectively) selected on the basis of a minimum 1.5-fold change and $p < 0.05$ (*t*-test) within a song nucleus were included. Pair-wise Pearson correlation coefficients were calculated for all genes selected. The resulting Pearson correlation matrix was transformed into a matrix of connection strengths (an adjacency matrix) using a power function $[(1 + \text{correlation})/2)^{\beta}]$, which was then converted to a topological overlap matrix. WGCNA identifies modules of densely interconnected probes by hierarchical clustering based on topological overlap, a biologically meaningful measure of similarity of expression patterns among all pairs of probes across all treatment conditions, and assigning each probe to a "module" based on shared expression patterns. A preliminary network was built to assess overall connectivity. From this network, the 6,500 and 3,800 probes in HVC and RA, respectively, with the highest connectivity were retained for subsequent WGCNA. For analysis using all expressed probes, I first omitted the probes with low connectivity (whole network connectivity; k.total < 0.5 and gray module) and then 32,607 probes in HVC and 21,669 probes in RA were used in the network construction. Modules were defined as branches of the dendrogram obtained from clustering and were labeled by colors beneath the dendrograms. To study the relationship between expression variability within the modules and behavioral trait variability, correlations were computed between principal components of each module and traits. *p* values were computed for each correlation.

3.3 Results

3.3.1 Gene expression dynamics in the motor circuit during song development

I used a whole genome strategy to evaluate gene expression dynamics in the motor circuit nuclei, HVC and RA, during the critical period of vocal learning in both intact and early-deafened birds. Global transcriptome profiling was performed using total RNA extracted from laser microdissected HVC and RA at three developmental stages: juvenile (dph 54–57), young adult (dph 121–135), and older adult (dph 504–787) (n = 3 deafened and intact birds at each developmental stage) (**Fig. III-1**). I used the songbird oligo-DNA array platform for comprehensive coverage of genes expressed in the zebra finch brain (Warren et al., 2010). After quality control assessment and normalization (see **Materials and Methods**), I surveyed 41,525 probes (11,391 gene-symbol identified genes) in HVC and 41,340 probes (11,374 genes) in RA of the 43,552 probe total set during at least one developmental period. I identified 3,362 probes in HVC (2,120 genes, 8.10% of the total HVC-expressed probes) and 1,466 probes in RA (974 genes, 3.54% of the total RA-expressed probes) that were differentially expressed during at least one developmental period (ANOVA, $p < 0.05$, **Fig. III-2**). These developmentally regulated genes encode signal transduction proteins, receptors, ion channels, cell adhesion molecules, neuron differentiation factors, and neuronal transcription factors, including *Sox4, Hey1, Znf238, Neurod6,* and *Mxi1* (**Fig. III-3**, **Fig. III-4**). In early-deafened birds, there were many fewer significant differences in expression between developmental periods in both HVC [1,922 of 2120 genes: 2,959 of 3,362 probes (88.0%)] and RA [915 of 974 genes: 1,357 of 1,466 probes (92.6%)], but individual variability in expression was also much higher as evidenced by the larger coefficient of variation (CV) compared with intact birds (**Fig. III-2, III-5**). This suggests that an underlying genetic program of developmental neural maturation continues after deafening, with auditory experience driving the stabilization of gene expression patterns and

levels. Nonetheless, examination of gene expression heat maps (**Fig. III-2)** shows similar gene expression patterns between groups and preservation of age-dependent expression dynamics in early-deafened birds. Nearly all genes [2,120 genes in HVC (100%) and 973 genes in RA (99.9%)] showed qualitatively similar intrinsic expression patterns during development, representing audition-independent robustness of gene expression dynamics in the motor circuit during song development. This robustness of gene expression dynamics is also indicated by similar average expression levels for most genes (**Fig. III-5**).

Indeed, the audition-independent robustness of age-dependent gene expression dynamics in the motor circuit could be demonstrated using the same set of genes (3,362 and 1,466 probes; in HVC and RA, respectively) by applying principal component analysis (PCA). I reduced the dimensionality of the gene expression pattern distribution by applying PCA to the collection of feature distributions of intact and early-deafened birds at three developmental stages (juvenile, young adult, and older adult), and the first three principal components (PC1, PC2, and PC3) were used to obtain the three-dimensional gene expression values. The PCs for gene expression values showed separable clusters for the three developmental stages but not for audition (+/−) in both HVC and RA (**Fig. III-6**). The core of each cluster was composed of intact individuals within the same age group surrounded by age-matched early-deafened individuals, indicating audition-independent, age-driven robust stability of gene expression programs but audition-dependent sensitivity that reduced expression fluctuation in the presence of auditory feedback.

To extract additional information on gene expression dynamics from the transcriptome dataset linked to developmental stage (age), audition (+/−), and song phenotype, I performed weighted gene co-expression network analysis (WGCNA) (Zhang and Horvath, 2005; Hilliard et al., 2012), which allows for the identification of “gene modules” of co-expressed genes.

Similar to PCA, WGCNA can also overcome a potential problem associated with the small sample sizes of the DNA microarray experiment because three developmental datasets were combined in both intact and deafened groups and used as a single dataset for the analysis (n = 18 in HVC and RA, separately). Within a set of genes that were differentially expressed to a significant level during at least one developmental stage both in intact and deafened birds (6,500 probes including 3,744 gene-symbol identified genes for HVC and 3,800 probes including 2,379 genes for RA), I identified 7 modules of co-expressed genes in HVC and 9 in RA (**Fig. III-7**). All gene modules in HVC (4,662 probes, 2,874 known genes) and 4 of 9 modules in RA (1,664 probes, 1,097 known genes) significantly correlated with the age-related parameters day post hatch and developmental stage. After Bonferroni correction, the first principal components of modules 1 and 2 in HVC (turquoise and blue, respectively, in **Fig. III-7**) were significantly related to age and motif consistency. The positive correlations of module 1 (2,620 probes representing 1,752 genes) in HVC indicate up-regulation of gene members during development. In contrast, module 2 (2,295 probes representing 1,353 genes) in HVC indicates a strongly negative correlation to age, and thus represents down-regulation of gene members during development. Module 1 (turquoise in **Fig. III-7**, 1,162 probes representing 816 genes) and module 3 (brown in **Fig. III-7**, 736 probes representing 496 genes) in RA also indicate significantly positive and negative correlations to age, respectively. Some of the gene modules, such as 1 and 2 in HVC and 7 in RA (black in **Fig. III-7**), also have weak but significant correlations with song parameters related to temporal regulation and syllable phonology. However, no gene module in either HVC or RA showed any significant correlation with auditory input. Likewise, no gene modules exhibited any significant correlation with auditory input in either HVC or RA when the data were reanalyzed using all expressed genes for WGCNA (using 41,525 and 41,340 probes for HVC and RA, respectively) instead of only using

the developmentally regulated subset. These results indicate the existence of audition-independent gene expression programs in the vocal motor circuit during song development at the co-expression network level.

3.3.2 Audition-independent gene expression dynamics associated with inevitable termination of vocal plasticity and acquisition of structured song patterns

The above results indicate a discrepancy between song phenotype variation and stable gene expression dynamics in the vocal motor circuit during development in the absence of auditory input. Song crystallization/stabilization, typically observed in the young adult stage (dph 100–120) in intact birds, was still observed in early-deafened birds but at older ages (>dph 300). However, the global gene expression pattern and level in the vocal motor circuit nuclei were quite similar between age-matched intact and deafened birds, and clearly different among the three developmental stages within these two groups. Thus, the gene expression pattern observed in the older adult stage (>dph 300) in both intact and deafened birds may be a molecular signature representing the “absolute” end-point of vocal plasticity associated with audition-independent vocal crystallization/stabilization. To examine this idea, I analyzed the long-term song stability following deafening after song pattern crystallization. Deafening young adult zebra finches induces deterioration of crystallized song patterns and results in variable song patterns (Nordeen, 1992; Lombardino and Nottebohm, 2000; Horita et al., 2008). This deterioration and instability of song pattern by adult auditory deprivation is considered the result of an output signal from the basal ganglia-forebrain circuit AFP, which detects mismatching of auditory feedback and vocal outputs, to the vocal motor circuit (Brainard and Doupe, 2000). However, instead of focusing on song deterioration, I examined whether unstable and variable song patterns continued or some degree of structured song pattern is eventually re-attained

because of an inherent decrease in vocal plasticity (i.e., if there is an age beyond which significant vocal plasticity cannot occur). I observed song deterioration and increased variability in song patterns one month after deafening in young adult birds (n = 4 at deafening operations were performed at dph 105–157; average dph 123.5). However, by dph 300–400 vocal variability started to decrease and song re-stabilized with a motif structure (**Fig. III-8**). The re-stabilized song was distinctly different from own first-crystallized song pattern and showed unique motif structure across birds (**Fig. III-8*A***). Individual song patterns once stabilized were repeatedly generated with the same temporal pattern, sequence, and phonologically deteriorated but stable syllables, resembling the songs of early-deafened birds.

Using a set of transcription factors that show developmentally different regulation in the motor circuit nuclei HVC and RA (**Fig. III-3, Fig. III-4**), I examined the gene expression patterns and levels in young adult-deafened birds during the song deterioration (more than a week after deafening, n = 5 at dph 104–161; average dph 132.4) and re-crystallization phases (n = 6 at dph 1158–1551; average dph 1274). I then compared these patterns with those of age-matched intact and early-deafened birds; however no significant differences in gene expression were observed in HVC and RA for any transcription factor examined among all age-matched, intact, early-deafened, and young adult deafened groups (**Fig. III-9**). These results support the idea of a genetic program-associated "absolute" end of vocal plasticity.

3.4 Discussion

Sensorimotor development is accelerated during critical periods of behavioral variation corresponding to enhanced neuroplasticity, followed by behavioral stabilization concomitant with reduced neuroplasticity. However, a certain degree of development and complex motor behavior may be achieved without the appropriate sensory inputs and may be driven by intrinsic developmental genetic programs instead.

Here, I revealed audition-independent vocal development and stabilization in a songbird zebra finch. Although our global transcriptome analysis identified over 3,000 genes differentially regulated in the vocal motor circuit during normal song development, I also observed similar qualitative patterns of developmental gene expression between the hearing-intact and early-deafened birds using PCA and WGCNA. Thus, vocal motor circuit maturation was driven by an audition-independent genetic mechanism. However, I cannot rule out the possibility that discrete effects of deafening on gene expression could be detected using other experimental designs (e.g., larger sample sizes, testing during singing instead of silence, testing at other developmental time points, or testing the AFP song nuclei). Adult-deafening reduces the size of dendritic spines and alters spontaneous action potential activity only in Area X projection neurons of HVC (Tschida and Mooney, 2012). Therefore, audition deprivation could alter developmental gene expression in a cell type-specific manner.

A few studies have examined the regulation of neural plasticity-related gene expression in the song system in social isolation-reared songbirds (Jin and Clayton, 1997a; Sakaguchi, 2004); however, to the best of our knowledge, the present study is the first to examine the dynamics of the brain transcriptome in a vocal learner under audition deprivation, a crucial epigenetic factor in vocal learning. It has been reported that several genes associated with song development are expressed in the song system during the critical period of song learning in

audition-intact birds (Soderstrom and Tian, 2006; Balmer et al., 2009; Kubikova et al., 2010). In addition, gene manipulation and pharmacological studies of motor circuit genes regulated by development reflect the effects on song development and song pattern generation (Denisenko-Nehrbass et al., 2000; Matsunaga et al., 2011). However, our global transcriptome analysis revealed a discrepancy between the dynamics of gene expression and song ontogeny, particularly during the young adult stage, when gene expression patterns were similar between the intact and deafened birds, but the stability of their song patterns considerably differed.

These results indicate two different regulations for the generation of a stable complex vocal pattern at the end of the critical period for vocal learning: auditory feedback-dependent “active” crystallization and “passive” crystallization associated with intrinsic developmental gene expression dynamics.

3.5 Figures

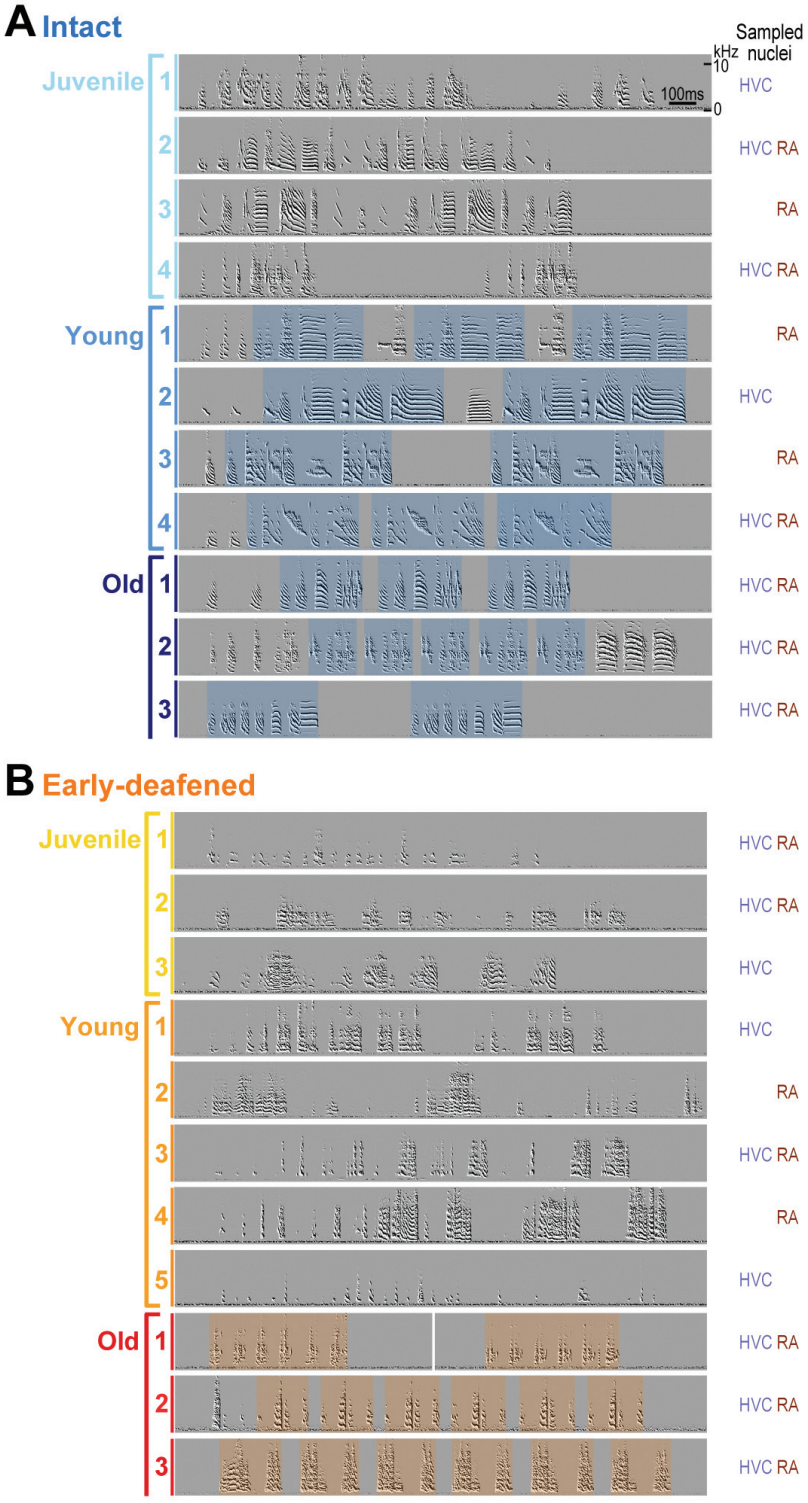
A Intact
Sampled nuclei
kHz
10
0
100ms
Juvenile
1
2
3
4
HVC
HVC RA
RA
HVC RA
Young
1
2
3
4
RA
HVC
RA
HVC RA
Old
1
2
3
HVC RA
HVC RA
HVC RA
B Early-deafened
Juvenile
1
2
3
HVC RA
HVC RA
HVC
Young
1
2
3
4
5
HVC
RA
HVC RA
RA
HVC
Old
1
2
3
HVC RA
HVC RA
HVC RA

Figure III-1. Song examples of the birds used for the DNA microarray experiment.

Color shadings highlight stable motifs. Right side of each spectrogram indicates the song nuclei laser microdissected for the microarray experiment.

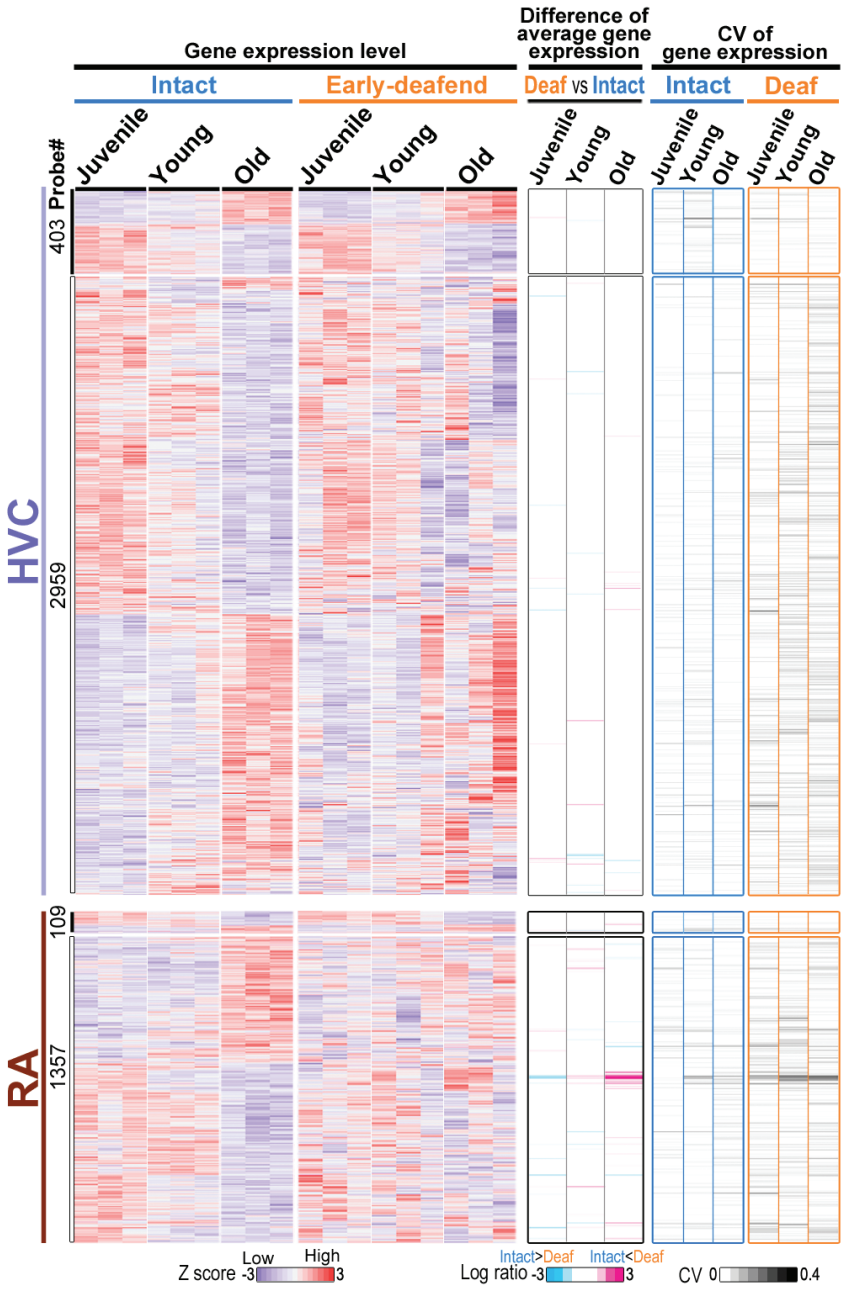
Gene expression level
Difference of average gene expression
CV of gene expression
Intact
Early-deafend
Deaf vs Intact
Intact
Deaf
Juvenile
Young
Old
Probe#
HVC
403
2959
RA
109
1357
Low
High
Z score -3
3
Intact>Deaf
Intact<Deaf
Log ratio -3
3
CV 0
0.4

Figure III-2. Gene expression dynamics in the motor circuit nuclei HVC and RA during development in intact and early-deafened zebra finches.

(Left: heat maps) Expression levels of 3,362 and 1,466 gene probes in HVC and RA, respectively, with significant differences across developmental stages in intact zebra finches (ANOVA, $p < 0.05$). The greater the absolute value of the Z score, the greater the gene's expression deviates from the mean,which indicates the significance of change in expression. The gene expression dynamics of early-deafened songbirds qualitatively represented a similar trend, but expression of the majority of these gene probes (2,959 in HVC and 1,357 in RA, white vertical bars) were no longer significantly different between developmental stages (ANOVA, $p < 0.05$). **(Middle column)** Differences in average gene expression level between intact and deafened birds at age-matched stages. **(Right columns)** Coefficient of variation (CV) of gene expression level for each gene probe at each developmental stage in intact and early-deafened birds.

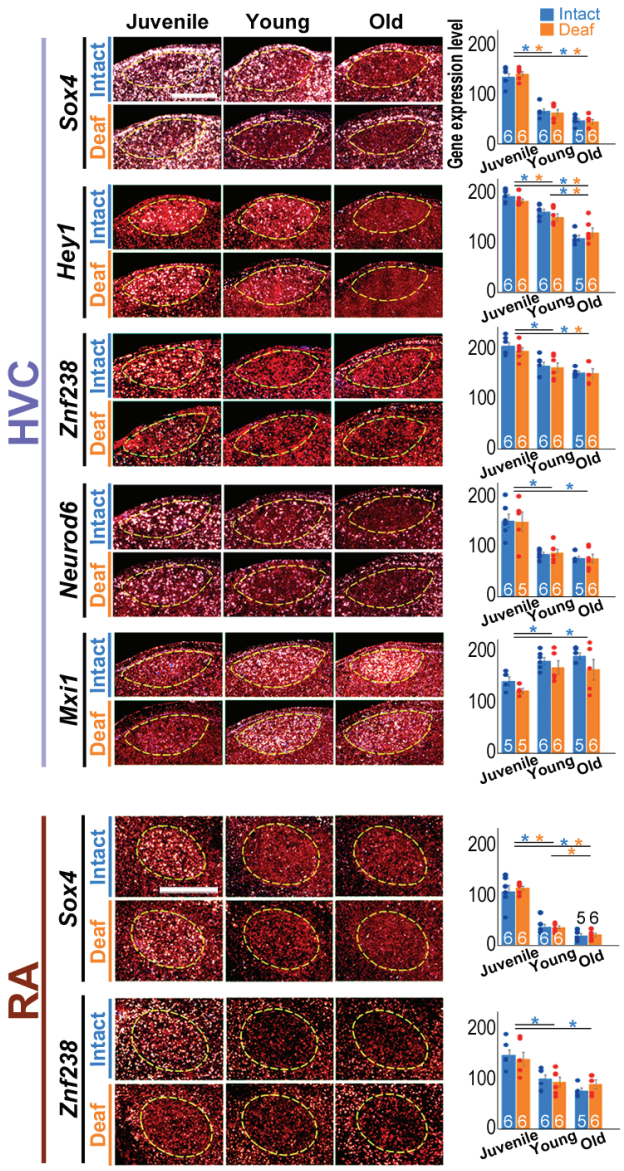
Juvenile
Young
Old
Intact
Deaf
Gene expression level
HVC
RA
Sox4
Hey1
Znf238
Neurod6
Mxi1
200
100
0
Juvenile
Young
Old

Figure III-3. Validation of mRNA expression levels of the differentially regulated transcription factors *Sox4*, *Hey1*, *Znf238*, *Neurod6*, and *Mxi1* in HVC and RA.

mRNA expression levels at three developmental stages for intact and early-deafened songbirds (juvenile: dph 47–59, young: dph 104–146, and old adult: dph 332–1715). White and red represent mRNA signal and Nissl counter-stained cells, respectively, in the sagittal brain section (right: anterior, up: dorsal). Scale bar = 1 mm. In intact birds, all genes examined were differentially regulated during development (*$p < 0.05$ after Bonferroni correction). In contrast, *Znf238*, *Neurod6*, and *Mxi1* expression levels were not significantly different between stages in early-deafened songbirds. Summarized bar graphs show the average gene expression level in each group (each animal number is indicated by inside bars). Each dot represents individual values (intact: blue, early-deafened: orange).

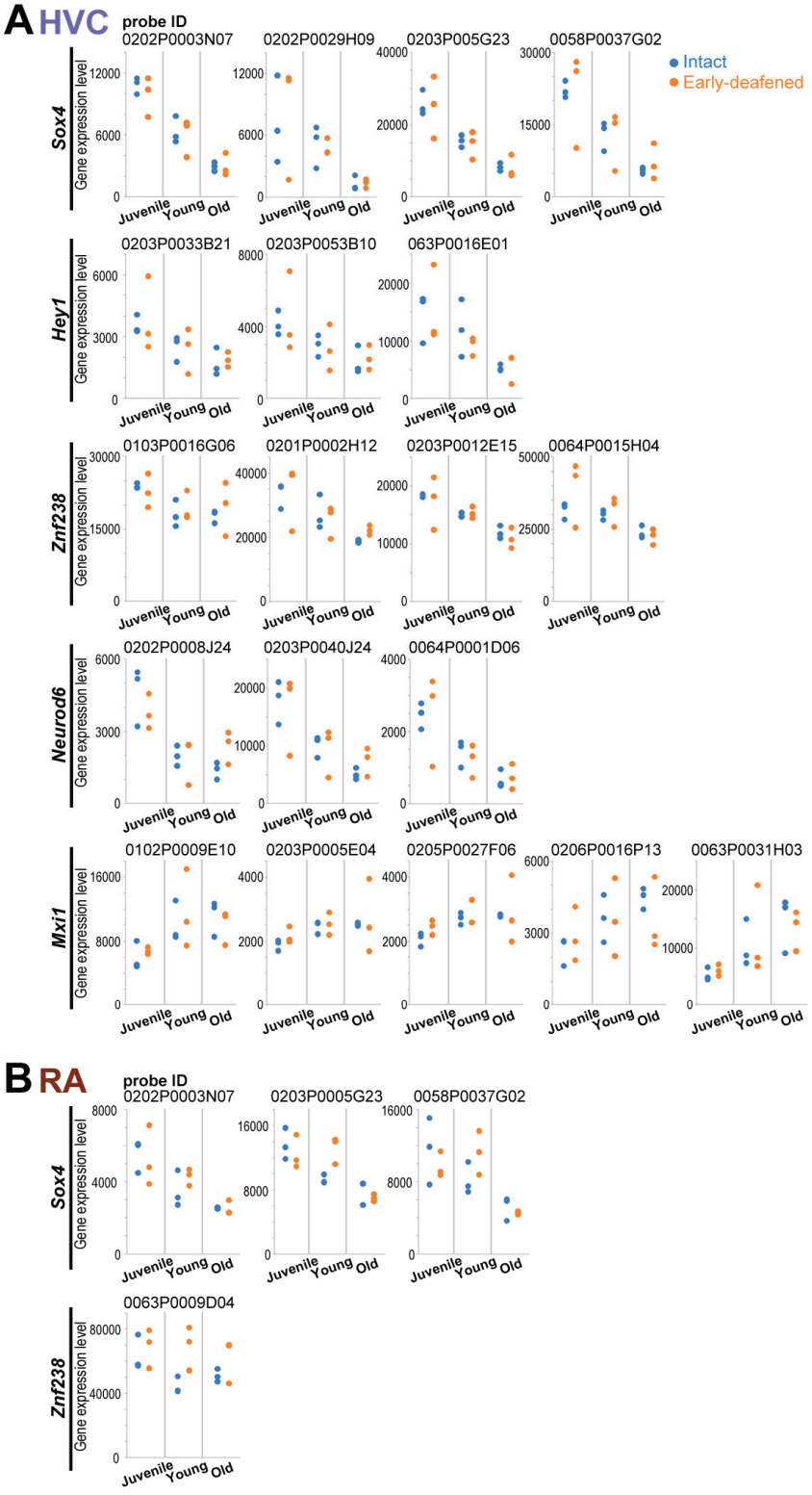
A HVC
probe ID
0202P0003N07
0202P0029H09
0203P005G23
0058P0037G02
Intact
Early-deafened
Sox4
Gene expression level
Juvenile
Young
Old
0203P0033B21
0203P0053B10
063P0016E01
Hey1
0103P0016G06
0201P0002H12
0203P0012E15
0064P0015H04
Znf238
0202P0008J24
0203P0040J24
0064P0001D06
Neurod6
0102P0009E10
0203P0005E04
0205P0027F06
0206P0016P13
0063P0031H03
Mxi1
B RA
probe ID
0202P0003N07
0203P0005G23
0058P0037G02
Sox4
0063P0009D04
Znf238

Figure III-4. Quantification of gene expression level by the DNA microarray.

Transcription factors, *Sox4*, *Hey1*, *Znf238*, *Neurod6*, and *Mxi1* used for expression validation by *in-situ* hybridization in **Fig. III-3** are indicated. Probe IDs are indicated at the top of the graph. Each plot indicates signal intensity from one bird. Juvenile: dph 47–59, young: dph 104–146, and old adult: dph 332–1715.

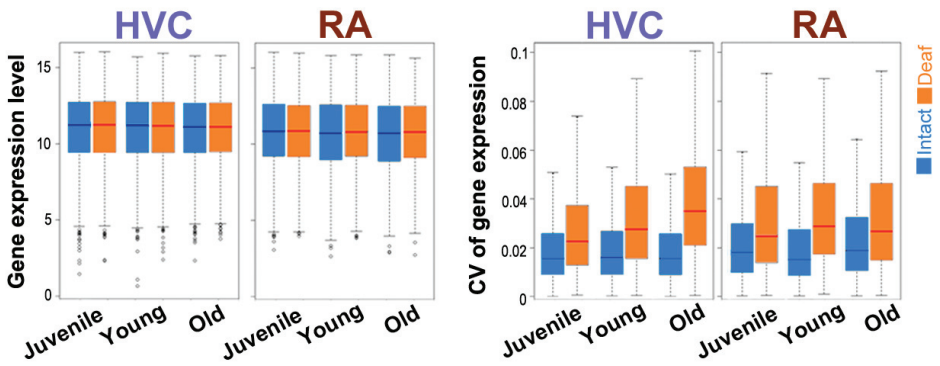
HVC
RA
Gene expression level
15
10
5
0
Juvenile
Young
Old
CV of gene expression
0.1
0.08
0.06
0.04
0.02
Intact
Deaf

Figure III-5. Gene expression level and CV of gene expression.

Gene expression level (left) and CV of gene expression (right) in HVC and RA at juvenile, young, and old adult stages in intact (blue) and early-deafened (orange) birds, using the same set of gene probes as shown in **Fig. III-2**. Each box illustrates median and interquartile range.

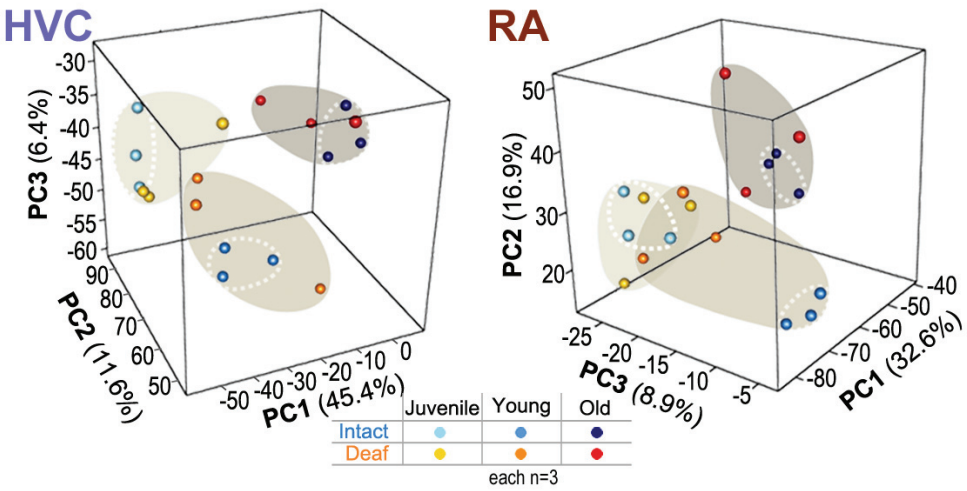
HVC
PC3 (6.4%)
-30
-35
-40
-45
-50
-55
-60
PC2 (11.6%)
90
80
70
60
50
PC1 (45.4%)
-50
-40
-30
-20
-10
0
RA
PC2 (16.9%)
50
40
30
20
PC3 (8.9%)
-25
-20
-15
-10
-5
PC1 (32.6%)
-40
-50
-60
-70
-80
Juvenile
Young
Old
Intact
Deaf
each n=3

Figure III-6. Gene expression dynamics in HVC and RA calculated by PCA using the same set of gene probes shown in Fig. III-2.

Beige shading indicates age-matched intact (light blue, blue, and dark blue) and early-deafened (yellow, orange, and red) groups.

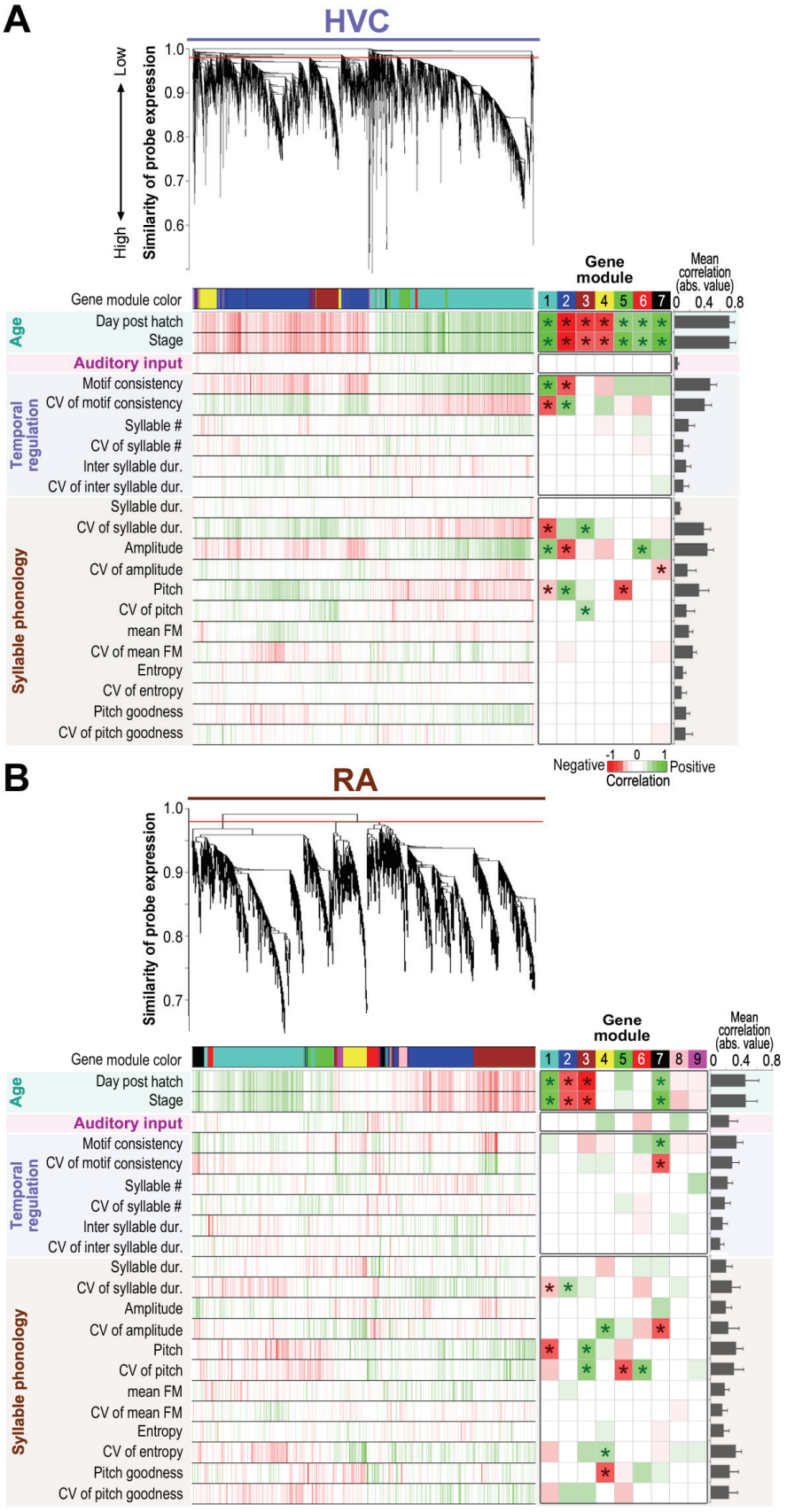
A
HVC
Similarity of probe expression
Low
High
1.0
0.9
0.8
0.7
0.6
Gene module
Mean correlation (abs. value)
Gene module color
1 2 3 4 5 6 7
0 0.4 0.8
Age
Day post hatch
Stage
Auditory input
Temporal regulation
Motif consistency
CV of motif consistency
Syllable #
CV of syllable #
Inter syllable dur.
CV of inter syllable dur.
Syllable phonology
Syllable dur.
CV of syllable dur.
Amplitude
CV of amplitude
Pitch
CV of pitch
mean FM
CV of mean FM
Entropy
CV of entropy
Pitch goodness
CV of pitch goodness
Negative
-1 0 1
Positive
Correlation
B
RA
Similarity of probe expression
1.0
0.9
0.8
0.7
Gene module
Mean correlation (abs. value)
Gene module color
1 2 3 4 5 6 7 8 9
0 0.4 0.8
Age
Day post hatch
Stage
Auditory input
Temporal regulation
Motif consistency
CV of motif consistency
Syllable #
CV of syllable #
Inter syllable dur.
CV of inter syllable dur.
Syllable phonology
Syllable dur.
CV of syllable dur.
Amplitude
CV of amplitude
Pitch
CV of pitch
mean FM
CV of mean FM
Entropy
CV of entropy
Pitch goodness
CV of pitch goodness

Figure III-7. Gene co-expression network analysis reveals strong correlations between gene modules and age-related factors but not with auditory input.

(Top) Dendrogram produced by average linkage hierarchical clustering of gene probes identifies 7 and 9 modules of co-expressed genes in HVC and RA, respectively. The red lines in the dendrograms indicate the height at which the tree was cut. Colored blocks denote individual gene modules.

(Bottom) Correlation between gene modules and age-, auditory input-, temporal regulation-, and syllable phonology-related parameters. Colored bands indicate positive (green) and negative (red) correlations. For each module (columns), heat maps show correlations to measured parameters (rows). Asterisks in each cell indicate significant trait relationships ($p < 0.05$, Student asymptotic *p*-values), for example, all 7 gene modules in HVC and 4 gene modules (module 1, 2, 3, and 7) in RA significantly correlate with the age-related parameters. Bar plots show average strength of module correlations to measured parameters (mean ± 95% confidence intervals).

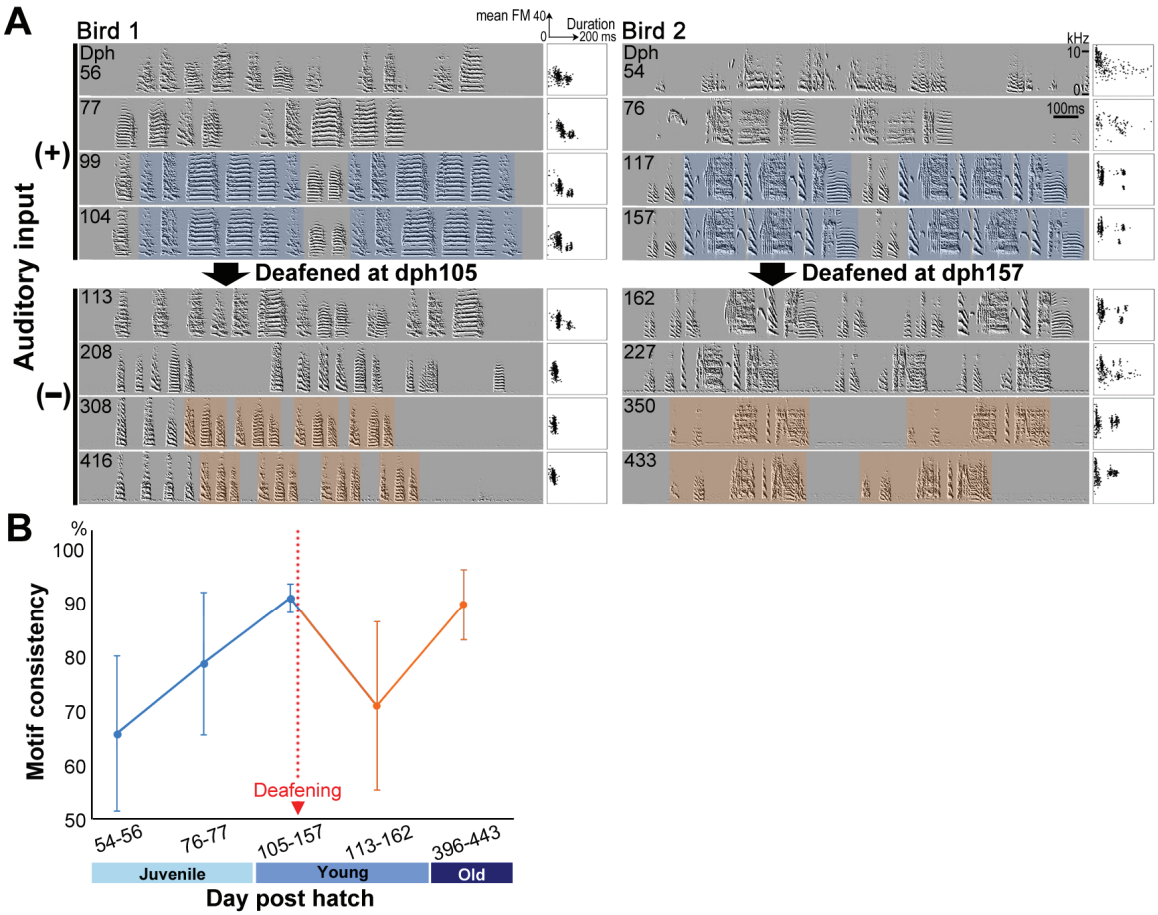
A
Bird 1
mean FM 40
0
Duration
200 ms
Bird 2
kHz
10
0
100ms
Dph
56
77
99
104
54
76
117
157
(+)
Auditory input
Deafened at dph105
Deafened at dph157
113
208
308
416
162
227
350
433
(−)
B
%
100
90
80
70
60
50
Motif consistency
Deafening
54-56
76-77
105-157
113-162
396-443
Juvenile
Young
Old
Day post hatch

Figure III-8. Zebra finches deprived of auditory input after song crystallization re-stabilize their song at old adult stage after deafening-induced song deterioration.

***A*,** Spectrograms of two example birds show song before and after adult-deafening. Songs re-stabilize without auditory input at old adult stage (orange shading in lower panels), i.e. the same period when early-deafened birds stabilize their song. Blue shading indicates the first crystallized songs developed at dph 100–150, with audition appearing before adult deafening.

***B*,** Change of motif consistency at each experimental stage before and after adult deafening (blue and orange spots, respectively; $n = 4$, mean ± SD). Motif consistency was calculated as the song similarity among 20 song motifs that were randomly selected at each developmental time point in each bird.

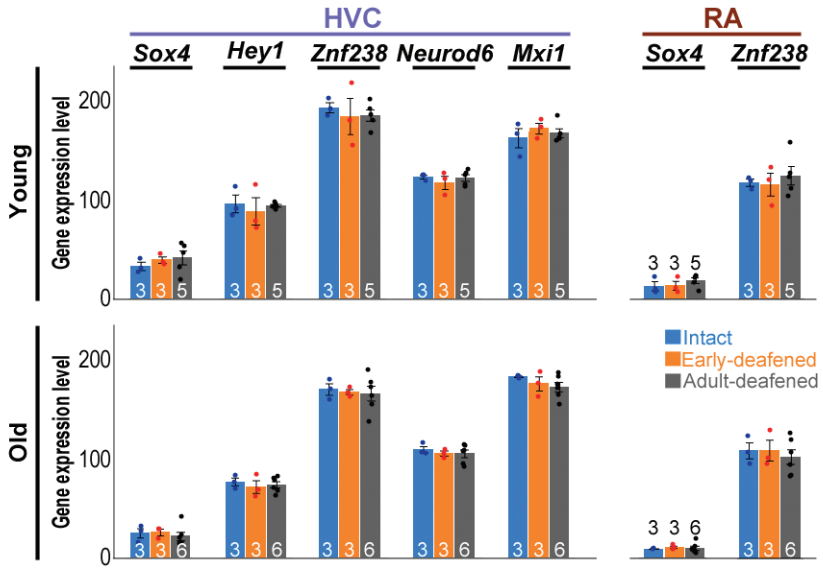
HVC
RA
Sox4
Hey1
Znf238
Neurod6
Mxi1
Sox4
Znf238
Young
Old
Gene expression level
200
100
0
3 3 5
3 3 6
Intact
Early-deafened
Adult-deafened

Figure III-9. mRNA expression levels of the developmentally regulated transcription factors *Sox4*, *Hey1*, *Znf238*, *Neurod6*, and *Mxi1* in HVC and RA.

Two developmental stages for intact, early-deafened, and young adult-deafened songbirds (young: dph 104–161, old adult: dph 1158–1551). Young adult-deafened operations were performed at dph 92–144. No significant difference was observed for any gene among the three groups at both stages (ANOVA, $p > 0.05$). Bar graphs show average the gene expression level in each group (each animal number is indicated by inside bars). Each dot represents individual value (intact: blue, early-deafened: orange, and young adult-deafened: black).

General Discussion

The ability of vocal learning is shared among several avian and mammalian lineages, including humans. Vocal learning involves the guidance of the animal's own vocal development by coordinating the sensory input to the motor output, and this is enabled by the auditory feedback of the produced sounds during a specific temporal window called the critical period. To understand the neural basis of vocal learning, a complex form of imitation, songbirds are good animal models because they are similar to humans in terms of behavior features and dedicated neural circuits for learned vocalization Studies of birdsong can help us understand how the development of neural circuits for vocal learning and production is driven by a sensory input (auditory information) and motor output (vocalization).

In this thesis, I used audition-deprived songbirds to examine the exact role of the auditory experience in the maturation of vocal learning and production-related neural circuits. In Chapter I, I have reported that the song eventually stabilizes with a species-typical structured pattern without auditory information. In Chapter II, I have shown that hearing loss does not affect the neural activity of the song nuclei in both the basal ganglia–forebrain circuit and the vocal motor circuit throughout vocal development. In Chapter III, I discovered audition-independent developmental gene expression dynamics in the vocal motor circuit throughout life which were time-locked in both hearing-intact and deafened birds. The results of my study provide new insights toward understanding the role of auditory input for vocal development, particularly with regard to the audition-independent robustness of song and neural maturation.

Based on our finding regarding audition-independent gene expression dynamics and the similar crystallization and re-crystallization timings of song both in the early- and adult-deafened birds, I propose a "two modes hypothesis" with "active" and "passive" modes that explains how song crystallization is regulated.

"Active" song crystallization is considered the traditional song crystallization maintained by the AFP using auditory feedback. In the zebra finch, this "active" crystallization is usually observed at approximately dph 90–120. Although the outward song pattern of a young adult appears stable after song crystallization, the global gene expression patterns in the song circuits sustain a level of neural plasticity that allows changes in vocal patterns at syllable, phonological, and sequential levels. Therefore, the neural plasticity associated with "active" crystallization was revealed by manipulating auditory feedback such as the delayed auditory feedback (Leonardo and Konishi, 1999) and deafening at the young adult stage in an AFP-dependent manner (Brainard and Doupe, 2000) (**Fig. III-8**). Furthermore, the neural plasticity associated with intrinsic gene expression patterns in a young adult would allow variable song patterns, with intervention of the AFP vocal exploration, but without evaluation of auditory feedback. An "active" crystallized song may contribute to mating for young adults because it acts as an early deceptive sign of individual maturation, just as the female-directed song is more stable than the undirected song and is therefore considered more attractive (Woolley and Doupe, 2008).

In contrast, late "passive" song crystallization would be independent of audition but associated with age- and/or singing experience, which emerges in the zebra finch at approximately dph 300. A previous experiment using adult-deafened zebra finches with a wide range of ages revealed a song deterioration that was more rapid in younger adults, whereas later-deafened adults showed few long-term changes in song structure (Lombardino and Nottebohm, 2000). The early- and adult-deafened birds revealed song stabilization and re-stabilization at approximately dph 300 (**Fig. I-1, III-8**). Furthermore, developmentally regulated gene expression patterns are similarly maintained in HVC and RA among the age-matched intact, early-, and adult-deafened birds (**Fig. III-2, III-7**). These results indicate the existence of an age- and/or singing experience-associated "passive" crystallization driven by

audition-independent gene expression dynamics in the vocal motor circuit.

There is no doubt about the importance of genomic information as the molecular basis for gene expression dynamics in acquiring species-specific vocal patterns. Although it is crucial to use auditory information to control song development, auditory-input is not the main driver of developmental gene expression dynamics in the motor circuit nuclei associated with audition-independent vocal crystallization in the zebra finch. Therefore, the audition-independent gene expression dynamics would provide a molecular signature for revealing an intrinsic state of neural plasticity in the song system. However, it remains necessary to examine the possible contribution of neural activity-driven epigenetic regulation of vocal development and the critical period in vocal learners.

Hearing impairment and developmental disabilities lead to deficits in acquired vocal patterns and maintenance during vocal development, including speech disorders, aphasias, and stuttering. Songbirds with experimentally disrupted auditory input are useful as animal models to help us understand how hearing impairment affects the development of brain regions for vocal learning and production. Although variability in the accuracy of syllable/word structures in children and adults with hearing impairments has been observed, little is known about the neural basis of this variability. Language outcomes may vary with the overall hearing level, age of onset of hearing loss, and therapeutic interventions, such as hearing aids or cochlear implants. In addition, vocal development may rely not only on how good one's hearing is but also on how much vocalization they produce. This suggests that interventions such as hearing aids or cochlear implants at an early stage of word production may have a more positive effect on language development in children with congenital hearing impairment.

Studies on birdsong, using behavioral manipulation and genetic and neurophysiological tools are shedding light on the vocal learning mechanisms by specialized neural networks.

Further research is required to understand how auditory input, motor activity, and aging affect the development of brain areas involved in vocal learning and production.

Acknowledgment

First of all, I would like to express my sincere gratitude to Dr. Kazuhiro Wada, my supervisor for giving me a great support, insightful comments and providing me a chance to collaborate with Dr Wan-chun Liu at the Rockefeller University. I learned not only molecular biological techniques but also how to passionately approach scientific questions.

I thank Dr. Wan-chun Liu (at the Rockefeller University) for providing me a chance to collect canary brains and for his great help in recording of canary. I also appreciate his critical comments on my study.

Special thanks also go to Drs. Toshiya Matsushima and Makoto Mizunami (at Hokkaido University) for their helpful comments and suggestions, and also for their patience as my thesis committee members.

I appreciate Dr. Aiko Watanabe for advice on the deafening operation; Dr. Andreas R. Pfenning (at Duke University) for providing gene annotations for the microarray; Drs. Haruhito Horita, Shin Yanagihara, and Satoshi Kojima for providing critical comments; Dr. Masayo Soma (at Hokkaido University) for her statistical advice; Dr. Kenta Suzuki for his advice on analysis using K-L distance; and Akiko Kamimura for her advice on how to perform the DNA microarray experiments; Akiko Ueno for helping with the analysis of canary song.

I appreciate members of laboratories of Animal Behavior and Intelligence for helping me to pursue my thesis research, especially Drs. Katsushi Kagaya, Ai Kawamori, Hidetoshi Amita,

and Yusuke Tomina for stimulating discussions and sympathetic support.

At Wada lab, I gratefully appreciate all lab members' help, especially Raimu Imai and Shin Hayase for helpful comments and supports on my thesis; Miguel Sanchez for correcting my English sentence.

I also appreciate the financial support of Japan Society for Promotion of Science that enabled me to complete my thesis.

Finally, I am deeply grateful to my parents for ungrudgingly supporting and their understanding of my Graduate School life.

References

Andalman AS, Fee MS (2009) A basal ganglia-forebrain circuit in the songbird biases motor output to avoid vocal errors. Proceedings of the National Academy of Sciences of the United States of America 106:12518-12523.

Aronov D, Andalman AS, Fee MS (2008) A specialized forebrain circuit for vocal babbling in the juvenile songbird. Science 320:630-634.

Balmer TS, Carels VM, Frisch JL, Nick TA (2009) Modulation of perineuronal nets and parvalbumin with developmental song learning. The Journal of neuroscience : the official journal of the Society for Neuroscience 29:12878-12885.

Bauer EE, Coleman MJ, Roberts TF, Roy A, Prather JF, Mooney R (2008) A synaptic basis for auditory-vocal integration in the songbird. The Journal of neuroscience : the official journal of the Society for Neuroscience 28:1509-1522.

Bottjer SW, Miesner EA, Arnold AP (1984) Forebrain lesions disrupt development but not maintenance of song in passerine birds. Science 224:901-903.

Brainard MS, Doupe AJ (2000) Interruption of a basal ganglia-forebrain circuit prevents plasticity of learned vocalizations. Nature 404:762-766.

Charlesworth JD, Warren TL, Brainard MS (2012) Covert skill learning in a cortical-basal ganglia circuit. Nature 486:251-255.

Denisenko-Nehrbass NI, Jarvis E, Scharff C, Nottebohm F, Mello CV (2000) Site-specific retinoic acid production in the brain of adult songbirds. Neuron 27:359-370.

Doupe AJ, Kuhl PK (1999) Birdsong and human speech: common themes and mechanisms. Annu Rev Neurosci 22: 567-631.

Eales LA (1985) Song learning in zebra finches: some effects of song model availability on what is learnt and when. Animal behaviour 33:1293-1300.

Egnor SER, Hauser MD (2004) A paradox in the evolution of primate vocal learning. TRENDS in neurosciences 27: 649-654.

Elliott KC, Wu W, Bertram R, Johnson F (2014) Disconnection of a basal ganglia circuit in juvenile songbirds attenuates the spectral differentiation of song syllables. Dev neurobiol 74: 574-590.

Erzurumlu RS, Gaspar P (2012) Development and critical period plasticity of the barrel cortex. The European journal of neuroscience 35:1540-1553.

Guo JU, Su Y, Zhong C, Ming GL, Song H (2011a) Hydroxylation of 5-methylcytosine by TET1 promotes active DNA demethylation in the adult brain. Cell 145:423-434.

Guo JU, Ma DK, Mo H, Ball MP, Jang MH, Bonaguidi MA, Balazer JA, Eaves HL, Xie B, Ford E, Zhang K, Ming GL, Gao Y, Song H (2011b) Neuronal activity modifies the DNA methylation landscape in the adult brain. Nature neuroscience 14:1345-1351.

Hahnloser RH, Kozhevnikov AA, Fee MS (2002) An ultra-sparse code underlies the generation of neural sequences in a songbird. Nature 419:65-70.

Hensch TK (2004) Critical period regulation. Annu Rev Neurosci 27:549-579.

Herrmann K, Arnold AP (1991) The development of afferent projections to the robust archistriatal nucleus in male zebra finches: a quantitative electron microscopic study. The Journal of neuroscience : the official journal of the Society for Neuroscience 11:2063-2074.

Hilliard Austin T, Miller Julie E, Fraley ER, Horvath S, White Stephanie A (2012) Molecular Microcircuitry Underlies Functional Specification in a Basal Ganglia Circuit Dedicated to Vocal Learning. Neuron 73:537-552.

Holtmaat A, Svoboda K (2009) Experience-dependent structural synaptic plasticity in the mammalian brain. Nat Rev Neurosci 10:647-658.

Horita H, Wada K, Jarvis ED (2008) Early onset of deafening-induced song deterioration and differential requirements of the pallial-basal ganglia vocal pathway. The European journal of neuroscience 28:2519-2532.

Horita H, Kobayashi M, Liu WC, Oka K, Jarvis ED, Wada K (2012) Specialized Motor-Driven dusp1 Expression in the Song Systems of Multiple Lineages of Vocal Learning Birds. PloS one 7:e42173.

Hubel DH, Wiesel TN (1970) The period of susceptibility to the physiological effects of unilateral eye closure in kittens. The Journal of Physiology 206:419-436.

Immelmann K (1969) Song development in the zebra finch and other estrildid finches. In: Bird Vocalizations (Hinde R, ed), pp 61–74. Cambridge: Cambridge University Press.

Janik VM, Slater PJB (1997) Vocal learning in mammals. Advances in the study of behavior 26: 59-99.

Jarvis ED (2004) Learned birdsong and the neurobiology of human language. Ann N Y Acad Sci 1016: 794-777.

Jarvis ED, Gunturkun O, Bruce L, Csillag A, Karten H, et al. (2005) Avian brains and a new understanding of vertebrate brain evolution. Nat Rev Neurosci 6: 151-159.

Jin H, Clayton DF (1997a) Synelfin regulation during the critical period for song learning in normal and isolated juvenile zebra finches. Neurobiology of learning and memory 68:271-284.

Jin H, Clayton DF (1997b) Localized changes in immediate-early gene regulation during sensory and motor learning in zebra finches. Neuron 19:1049-1059.

Jones MW, Errington ML, French PJ, Fine A, Bliss TV, Garel S, Charnay P, Bozon B, Laroche S, Davis S (2001) A requirement for the immediate early gene Zif268 in the expression of late LTP and long-term memories. Nature neuroscience 4:289-296.

Kao MH, Doupe AJ, Brainard MS (2005) Contributions of an avian basal ganglia-forebrain circuit to real-time modulation of song. Nature 433:638-643.

Knudsen EI (2004) Sensitive periods in the development of the brain and behavior. Journal of cognitive neuroscience 16:1412-1425.

Kojima S, Kao MH, Doupe AJ (2013) Task-related "cortical" bursting depends critically on basal ganglia input and is linked to vocal plasticity. Proceedings of the National Academy of Sciences of the United States of America.

Konishi (1964) Effects of deafening on song development in two species of juncos. The Condor 66:85-102.

Konishi M (1965) Effects of deafening on song development in American robins and black-headed grobeaks. Zeitschrift fur Tierpsychologie 22:584-599.

Konishi M (1965) The role of auditory feedback in the control of vocalization in the white-crowned sparrow. Zeitschrift fur Tierpsychologie 22:770-783.

Konishi M (1985) Birdsong: From behavior to neuron. Ann Rev Neurosci 8: 125-170

Kroodsma DE, Pickert R (1984) Sensitive phases for song learning: Effects of social interaction and individual variation. Animal behaviour 32:389-394.

Kubikova L, Wada K, Jarvis ED (2010) Dopamine receptors in a songbird brain. The Journal of comparative neurology 518:741-769.

Langfelder P, Horvath S (2008) WGCNA: an R package for weighted correlation network analysis. BMC bioinformatics 9:559.

Leonardo A, Konishi M (1999) Decrystallization of adult birdsong by perturbation of auditory feedback. Nature 399:466-470.

Li X, Wang XJ, Tannenhauser J, Podell S, Mukherjee P, Hertel M, Biane J, Masuda S, Nottebohm F, Gaasterland T (2007) Genomic resources for songbird research and

their use in characterizing gene expression during brain development. Proceedings of the National Academy of Sciences of the United States of America 104:6834-6839.

Li XC, Jarvis ED, Alvarez-Borda B, Lim DA, Nottebohm F (2000) A relationship between behavior, neurotrophin expression, and new neuron survival. Proceedings of the National Academy of Sciences of the United States of America 97:8584-8589.

Lombardino AJ, Nottebohm F (2000) Age at deafening affects the stability of learned song in adult male zebra finches. The Journal of neuroscience : the official journal of the Society for Neuroscience 20:5054-5064.

Ma DK, Jang MH, Guo JU, Kitabatake Y, Chang ML, Pow-Anpongkul N, Flavell RA, Lu B, Ming GL, Song H (2009) Neuronal activity-induced Gadd45b promotes epigenetic DNA demethylation and adult neurogenesis. Science 323:1074-1077.

Mahrt EJ, Perkel D, Tong L, Rubel EW, and Portfors CV (2013) Engineered deafness reveals that mouse courtship vocalizations do not require auditory experience. The Journal of neuroscience : the official journal of the Society for Neuroscience 33:5573-5583.

Majdan M, Shatz CJ (2006) Effects of visual experience on activity-dependent gene regulation in cortex. Nature neuroscience 9:650-659.

Marler P (1970) A comparative approach to vocal learning: Song development in white-crowned sparrows. Journal of Comp Phyiol Psychol Monograph 71:1-25

Marler P, Mundinger P, Waser MSs, and Lutjen A (1972) Effects of acoustical stimulation and deprivation on song development in red-winged blackbirds (*Agelaius phoeniceus*). Animal Behaviour 20:586-606.

Marler P, Slabbekoorn H. (2004) Nature's music: The science of birdsong. Elsevier.

Marler P, Waser MS (1977) Role of auditory feedback in canary song development. Journal of Comparative and Physiological Psychology 91:8-16.

Marler P, Sherman, V. (1983) Song structure without auditory feedback: emendations of the auditory template hypothesis The Journal of Neuroscience 3:517-531.

Matsunaga E, Suzuki K, Kato S, Kurotani T, Kobayashi K, Okanoya K (2011) Dynamic expression of cadherins regulates vocal development in a songbird. PloS one 6:e25272.

Meaney MJ, Ferguson-Smith AC (2010) Epigenetic regulation of the neural transcriptome: the meaning of the marks. Nature neuroscience 13: 1313-1318.

Michod D, Bartesaghi S, Khelifi A, Bellodi C, Berliocchi L, Nicotera P, Salomoni P (2012) Calcium-Dependent Dephosphorylation of the Histone Chaperone DAXX Regulates H3.3 Loading and Transcription upon Neuronal Activation. Neuron 74:122-135.

Nordeen K, Nordeen, E (1992) Auditory Feedback is Necessary for the Maintenance of Stereotyped Song in Adult Zebra FInches. Behavioral and Neural Biology 57:58-66.

Nottebohm, F (1968) Auditory experience and song dvelopment in the chaffinch *Fringilla coelebs*. Ibis 110:549-568

Nowicki S, Searcy WA, Peters S (2002) Brain development, song learning and mate choice in birds: a review and experimental test of the "nutritional stress hypothesis". Journal of comparative physiology A, Neuroethology, sensory, neural, and behavioral physiology 188:1003-1014.

Ölveczky B, Andalman, AS., Fee MS (2005) Vocal Experimentation in the Juvenile Songbird Requires a Basal Ganglia Circuit. PLoS biology 3:e153.

Poole JH, Tyack PL, Stoeger-Horwath AS, Watwood S (2005) Animal behaviour: Elephants are capable of vocal learning. Nature 434: 455-456.

Poopatanapong A, Teramitsu I, Byun JS, Vician LJ, Herschman HR, White SA (2006) Singing, but not seizure, induces synaptotagmin IV in zebra finch song circuit nuclei.

Journal of neurobiology 66:1613-1629.

Price P (1979) Developmental Deterrninants Of Structure in Zebra Finch Song. Jounral of Comprative and Physiological Psychology 93:260-277.

Replogle K et al. (2008) The Songbird Neurogenomics (SoNG) Initiative: community-based tools and strategies for study of brain gene function and evolution. BMC genomics 9:131.

Riccio A (2010) Dynamic epigenetic regulation in neurons: enzymes, stimuli and signaling pathways. Nature neuroscience 13: 1330-1337.

Ruben RJ (1997) A time frame of critical/sensitive periods of language development. Acta oto-laryngologica 117:202-205.

Sakaguchi H (2004) Effect of social factors on the development of PKC expression in songbird brain. Neuroreport 15:2819-2823.

Scharff C, Nottebohm F (1991) A comparative study of the behavioral deficits following lesions of various parts of the zebra finch song system: implications for vocal learning. The Journal of neuroscience : the official journal of the Society for Neuroscience 11:2896-2913.

Soderstrom K, Tian Q (2006) Developmental pattern of CB1 cannabinoid receptor immunoreactivity in brain regions important to zebra finch (Taeniopygia guttata) song learning and control. The Journal of comparative neurology 496:739-758.

Stark LL, Perkel DJ (1999) Two-stage, input-specific synaptic maturation in a nucleus essential for vocal production in the zebra finch. The Journal of neuroscience : the official journal of the Society for Neuroscience 19:9107-9116.

Tchernichovski O, Nottebohm F (1998) Social inhibition of song imitation among sibling male zebra finches. Proceedings of the National Academy of Sciences of the United

States of America 95:8951-8956.

Tchernichovski O, Nottebohm F, Ho CE, Pesaran B, Mitra PP (2000) A procedure for an automated measurement of song similarity. Animal behaviour 59:1167-1176.

Teramitsu I, Poopatanapong A, Torrisi S, White SA (2010) Striatal FoxP2 is actively regulated during songbird sensorimotor learning. PloS one 5:e8548.

Tschida Katherine A, Mooney R (2012) Deafening Drives Cell-Type-Specific Changes to Dendritic Spines in a Sensorimotor Nucleus Important to Learned Vocalizations. Neuron 73:1028-1039.

Van der Loos H, Woolsey TA (1973) Somatosensory cortex: Structural alterations following early injury to sense organs. Science 26:395-398.

Wada K, Sakaguchi H, Jarvis ED, Hagiwara M (2004) Differential expression of glutamate receptors in avian neural pathways for learned vocalization. The Journal of comparative neurology 476:44-64.

Wada K, Howard JT, McConnell P, Whitney O, Lints T, Rivas MV, Horita H, Patterson MA, White SA, Scharff C, Haesler S, Zhao S, Sakaguchi H, Hagiwara M, Shiraki T, Hirozane-Kishikawa T, Skene P, Hayashizaki Y, Carninci P, Jarvis ED (2006) A molecular neuroethological approach for identifying and characterizing a cascade of behaviorally regulated genes. Proceedings of the National Academy of Sciences of the United States of America 103:15212-15217.

Warren WC et al. (2010) The genome of a songbird. Nature 464:757-762.

Woolley SC, Doupe AJ (2008) Social context-induced song variation affects female behavior and gene expression. PLoS biology 6:e62.

Wu W, Thompson JA, Bertram R, Johnson F (2008) A statistical method for quantifying songbird phonology and syntax. Journal of neuroscience methods 174:147-154.

Yu AC, Margoliash D (1996) Temporal hierarchical control of singing in birds. Science 273:1871-1875.

Zann RA (1996) The Zebra Finch: a Synthesis of Field and Laboratory Studies. Oxford: Oxford University Press:198-247.

Zhang B, Horvath S (2005) A general framework for weighted gene co-expression network analysis. Statistical applications in genetics and molecular biology 4:Article17.

List of Publications

Chihiro Mori and Kazuhiro Wada:

"Audition-independent vocal crystallization associated with intrinsic developmental gene expression dynamics."

Journal of Neuroscience, vol. 35, No. 3, pp.878-889 (2015)

List of Other Publications

1. Kazuhiro Wada, Shin Hayase, Raimu Imai, Chihiro Mori, Masahiko Kobayashi, Wan-chun Liu, Miki Takahasi and Kazuo Okanoya:
   "Differential androgen receptor expression and DNA methylation state in striatum song nucleus Area X between wild and domesticated songbird strains."
   European Journal of Neuroscience, vol. 38, No. 4, pp.2600-2610 (2013)

2. 今井礼夢，森千紘，和多和宏:
   "ソングバードの囀りを制御する神経回路・遺伝子"
   生物の科学　遺伝，11 月号 (2010)

3. 森千紘，和多和宏:
   "ヒト以外の動物にことばはあるかーヒトの言語とソングバードの囀りー"
   JOHNS，8 月号 (2011)